Investigating the Functions of the Plant-associated Genus *Variovorax* in the *Populus* Rhizosphere

A Thesis Presented for the

Master of Science

Degree

The University of Tennessee, Knoxville

Jennifer Ann Childers

December 2019

ACKNOWLEDGEMENTS

I would like to thank my ever-supportive advisor, Dr. Jenny Morrell-Falvey, for the continual guidance to dig deeper and go further with my project. Her expertise and encouragement have been invaluable to my training as a scientist. I would also like to thank Dr. Amber Bible Webb for the continued help and advice she frequently offered in the lab. Thank you to the Genome Science and Technology program and the Plant Microbe Interface group at Oak Ridge National Laboratory for this opportunity. Thank you to my committee members Dr. Gladys Alexandre, Dr. Sarah Lebeis, and Dr. Dale Pelletier for their advice in shaping my project. Lastly, I would like to thank my family and friends for their continued support and encouragement throughout my time in the program.

ABSTRACT

Plants host a diverse microbial community living in close association with their roots (rhizosphere) or inside plant tissues (endosphere) that can form beneficial, pathogenic, or neutral relationships. Understanding these relationships can inform strategies for manipulating the microbiome of plants to promote plant growth and productivity. Among the microbes isolated and sequenced from the *Populus* rhizosphere and endosphere are a number of *Variovorax* isolates. *Variovorax* ssp. are motile, Gram-negative bacteria that belong to the family *Comamonadaceae* and are known for their diverse metabolism. For this work, we characterized thirteen new *Populus*-associated *Variovorax* strains, twelve of which were isolated from the endosphere and one from the rhizosphere of *Populus*. Genomic comparisons indicate that these isolates encode a high level of genomic and metabolic diversity. We have performed assays to characterize interactions between *Variovorax* and other bacterial strains, examined biosurfactant production, and performed genome analyses to predict biosynthetic gene clusters for natural product production by the *Variovorax* species. Despite being isolated from a common host, these analyses indicate that the *Populus*-associated *Variovorax* strains show variations in metabolic potential, in their interactions, in the diversity and abundance of biosynthetic gene clusters, and in biosurfactant production.

TABLE OF CONTENTS

LIST OF TABLES

LIST OF FIGURES

CHAPTER ONE :
BACKGROUND

The Plant Microbiome

The rhizosphere is comprised of a complex assemblage of microbes that forms an interface between plant roots and the large biodiversity of microbes growing in bulk soil.[1,2] At present, bacteria are thought to be recruited from bulk soil to the rhizosphere based on their attraction to compounds in root exudates that are produced by the plant and released into the soil.[3-5] Root exudates are byproducts of photosynthetically fixed carbon and consist of a wide variety of molecules such as organic acids, amino acids, carbohydrates, and vitamins which can be used for growth by bacteria.[6,7]

Many soil bacteria have the ability to sense and respond to the chemicals from root exudates using the process of chemotaxis. Chemotaxis involves binding of chemical stimuli to methyl-accepting chemotaxis proteins (MCPs) that are receptors on bacterial cells.[8] This process involves a conserved signaling cascade that includes the proteins CheA, CheY, CheW, CheB, and CheR.[9] The histidine kinase CheA is bound to the MCPs by CheW and becomes autophosphorylated.[9] The phosphoryl group is then transferred to CheY which causes a reversal in flagellar movement, from counterclockwise to clockwise, allowing the bacterium to reorient its cell body by tumbling.[9] After the initial perception, CheR and CheB tune the receptor methylation to either increase or decrease the activity of CheA, respectively.[9] Through alternating bacterial runs with tumbling, the bacteria can explore their environment by randomly changing directions.[10] Once a chemical gradient is sensed, bacteria can bias their random walk to lengthen their swimming runs in an up-gradient direction towards chemical attractants.[10] Without chemotaxis, some bacteria have reduced movement toward specific root exudates as well as reduced root colonization even if motile.[11] For example, early colonization of roots by *Bacillus subtilis*

depends on chemotaxis which involves the binding of amino acids secreted from the plant to MCPs of the bacteria.[12] Many bacteria that are able to use chemotaxis can perceive plant root exudates, allowing for the eventual movement of the bacteria toward the plant.

Once recruited to the plant microbiome, the bacteria will be within the zone of influence of the plant. While many bacteria will remain in the rhizosphere and colonize the plant root surface, another subset will enter the plant and become part of the endosphere.[13,14] How bacteria are able to enter the plant for colonization is unknown for most endophytes, although evidence for using root cracks, lateral root formation points, or cell wall degrading enzymes, such as endoglucanase, has emerged.[15] However, the mechanism for endosphere colonization by nodulating bacteria is well characterized. The nodulating bacteria perceive flavonoids produced by the plant, causing colonization of the root hair. Once colonized, the release of Nod factors by the bacteria cause the root hair to curl, entrapping the bacteria. Simultaneously, an infection thread grows which allows the bacteria into the plant and the growth of the nodule is eventually produced by the plant.[16]

As members of the plant microbiome, bacteria can influence plant health and productivity by forming beneficial, pathogenic, or neutral relationships with the plant.[17] The type of relationship that the bacteria forms depends on the type of characteristics the bacteria possess. Common beneficial characteristics that lead to plant growth promotion include phytohormone production, secondary metabolite production, nitrogen fixation, or biocontrol of pathogens.[18] In addition, beneficial plant-microbe interactions can help during abiotic or biotic stress conditions, mitigating loss of growth that occurs during environmental stress.[19-21]

The structure of the microbiome, such as the diversity, abundance, and spatial distribution of microbes, is constantly in flux. Research into determining what factors affect community structure has grown in recent years. For example, a study in which three different plants species, *Populus, Quercus,* and *Pinus,*

were grown in a common soil showed that the microbiome composition for *Populus* was significantly different than the microbiome composition of *Quercus* and *Pinus,* suggesting that the plant host has significant effect on the microbes found within its microbiome.[22] Another study looking at how tree species diversity and richness from mixed and mono stands influences bacterial composition found that the tree species is significant in determining the microbiome composition and to a lesser extent the richness of the species in a mixed stand.[23]

Additionally, environmental conditions can impact the structure of the microbiomes. While no single condition can explain the variability between different microbiome structures, there are, however, a few common conditions that have significant effects on the diversity and abundance of microbial taxa within the microbiome.[24] For example, the pH of soil is one of the most influential characteristics for determining the structure of microbiomes when a broad range of soil pHs (between pH 4 and pH 8) are collected and analyzed.[25,26] Available nutrients within the soil, such as soil organic carbon and nitrogen, also affects the abundance of certain microbes within the microbiome.[27,28] Likewise, the temperature at which a microbial community is grown will affect its structure. Analysis of a core group of microbes across different soil types demonstrated similar and predictable responses to changing temperatures.[29] Furthermore, alteration to the compounds found within the microbiome will affect the microbial abundance and diversity. The composition of root exudates has been shown to alter with age in *Arabidopsis,* as well as individual *Arabidopsis* genotypes producing a unique root exudate profile.[30,31] Differences in the root exudation patterns have, in turn, been shown to influence the microbiome assemblages for the plant.[32] Evidence of secreted metabolites from microbes can alter root exudates in the plant, suggesting an indirect effect by microbes on community structure.[33] However, microbially secreted metabolites can also have a direct effect by acting as signaling molecules, growth substrates for other bacteria, and for outcompeting other microbes.[34] Understanding the ways in which individual

bacterial strains can influence the community structure is still largely uncharacterized.

The *Populus* Microbiome

Populus is a fast growing woody perennial with potential to be utilized as a renewable source of biofuels and bioproducts.[35] These trees can be grown on land that is unsuitable for growing food crops and *Populus* increases carbon sequestration which reduces the carbon debt that occurs from land use changes.[36] Additionally, *Populus* was the first tree to have its genome sequenced and microbiome characterized.[35-37] Analysis of the microbiome has demonstrated that *Populus* hosts two distinct bacterial populations between its rhizosphere community and endosphere community.[36] The rhizosphere community is more diverse than its endosphere and dominated by *Acidobacteria* and *Alphaproteobacteria* while the endosphere is dominated by *Gammaproteobacteria* and *Alphaproteobacteria*.[36,37] Additionally, the metabolic functions of closely related bacteria isolated from the endosphere can differ compared to bacteria isolated from the rhizosphere. For example, *Pseudomonas fluorescens* strains isolated from the *Populus* endosphere had significantly more metabolic pathways for plant signaling, were biased toward utilizing nucleotides and sugars, and displayed more plant growth promoting traits compared to rhizosphere isolates that had more metabolic pathways for root exudates but less pathways related to plant-microbe interactions.[38] Abiotic conditions have also been shown to shift the *Populus* microbiome; with season, geography, and soil pH causing variance in the abundance and diversity of microbes collected at a particular time and place.[37]

Recent work has examined how individual environmental factors affect members of the *Populus* microbiome. *Populus* grown under abiotic stress conditions have been shown to alter the microbes within the microbiome. Furthermore, a subset of bacterial strains became enriched regardless of the

stressor, suggesting a core stress microbiome during abiotic stressors.[39] The characteristics of the soil also has an influential role in the microbiome structure. When microbes are grown in several different soils, differing in either its origins or properties, and using several *Populus* genotypes, the soil origin plays a larger role in the microbiome structure than the genotype, although genotype is also important.[40,41]

Natural Products

While characterization of the plant microbiome has increased, there is still a lack of information regarding secreted metabolites produced by the microbiome members. Secreted metabolites, known as natural products or secondary metabolites, are molecules that are not necessary for growth and are typically produced as nutrients become limited.[34] Natural products cover a few defined classes of molecules but can range in variety of structures due to variations in production mechanisms, building blocks, and processing.[34] Despite not being necessary for growth, bacterially produced natural products have many ecological benefits for the bacteria in their communication with other bacteria within the microbiome.[34] Possible ecological roles include molecules that act to inhibit growth of other bacterial strains, stimulate sporulation, signaling molecules, compounds that lead to plant growth promotion, molecules that can help to increase motility and biofilm formation in the bacteria, and alter gene expression.[34]

Genes related to natural product production are often found in biosynthetic gene clusters which can be identified through genome mining and lab screening for the expected compound.[42] One challenge to natural product discovery is identifying which genes encode a product as many biosynthetic gene clusters are not expressed under laboratory conditions.[43] Because these products may play a role in native environments, some clusters can be activated through growing bacteria in the presence of another microbial strain.[43] For example, growing

Streptomyces species with *Tsukamurella pulmonis* TP-B0596 resulted in the discovery of a unknown red pigment as well as a novel antibiotic.[44] The mycolic acid production by *T. pulmonis* is thought to alter the environmental conditions which, in turn, alter the secondary metabolism of the *Streptomyces* species.[44] Utilizing these and other methods to activate biosynthetic gene clusters provides a promising future for discovering novel natural products.

The biosynthetic potential for the *Populus* microbiome was recently characterized by Blair et al. Over 3,400 biosynthetic gene clusters were identified from 339 sequenced *Populus* isolates.[45] The gene clusters range in diversity over the natural product categories, with many being unique. Less than 1% of the identified gene clusters matched to a previously characterized gene cluster.[45] Therefore, future research into the potential for natural product production in the *Populus* microbiome could lead to wealth of novel molecules.

Biosurfactants

Surfactants are amphiphilic compounds that can reduce surface tension of a liquid on surfaces or at the interface of two liquids.[46] They can act as foaming and dispersing agents, emulsifiers, and detergents, making them ideal for many commercial processes including cleaning materials, food processing, and petroleum production.[47,48] However, synthetic surfactants pose potential environmental harm as they are non-biodegradable.[49] Microbially produced biosurfactants are typically biodegradable, less toxic and have similar properties as synthetic surfactants, making them a promising option for replacing synthetic surfactants.[50]

Biosurfactants range in size and shape, with many being branched or cyclic in structure.[51] They are broadly characterized into six types: glycolipids, lipopeptides, phospholipids, fatty acids or natural lipids, polymeric surfactants, or particulate surfactants.[47,52] While a variety of bacterial genera produce biosurfactants, research has largely focused on the lipopeptides, particularly

rhamnolipids produced by *Pseudomonas* strains and surfactin produced by *Bacillus* strains.[46] These lipopeptides are synthesized by nonribosomal peptide synthetases (NRPSs), which uses a thiotemplate process.[53] However, other biosurfactants, such as the inturin family, use a different, hybrid system for synthesis that includes a polyketide synthase (PKS) in addition to a NRPS to form the hybrid PKS/NRPS biosynthetic system.[54] Additionally, two-component systems and quorum sensing are common biosurfactant production regulation schemes for *Bacillus* and *Pseudomonas*.[46]

Biosurfactants have been shown to contribute to several microbial behaviors that help microbes in their native environments. Surfactin and rhamnolipid production in *Bacillus* and *Pseudomonas*, respectively, are necessary for swarming motility by acting as a wetting agent on a surface.[55,56] Biosurfactants also contribute to normal biofilm formation and maintenance. For example, characterization of a *P. aeruginosa* mutant deficient in biosurfactant production showed that this mutant produced biofilms that lacked water channels, but maintained the thickness of a biofilm compared to wild type.[57] *B. subtilis,* on the other hand, requires surfactin to form normal pellicles, a type of biofilm that forms at the air-liquid interface.[58] Research into the antimicrobial properties of biosurfactants has shown that they can affect a broad range of microbes, including gram positive and gram negative bacteria and fungi.[59]

Therefore, biosurfactant production likely influences interactions with other microbes and the host plant, suggesting that biosurfactant production may play a role in plant colonization and microbiome dynamics. Biosurfactants are thought to promote plant growth by increasing the wettability of the soil and through antimicrobial properties. The increased wettability of the soil by secreted biosurfactants could contribute to increasing colonization of microbes with the plant roots. Recently, research has suggested that a bacterial strain that coexists beneficially with a biosurfactant-producer can utilize the biosurfactant molecules to help their own motility and degrade the biosurfactant molecules to use as

territory markers.[60] Additionally, antimicrobial properties can influence community structure by impacting which microbes can successfully colonize and become a part of the plant microbiome.[61] Lastly, some biosurfactants have the ability to disrupt the biofilms of other bacteria. Rhamnolipids have been shown to disrupt the biofilms of a variety of bacteria and prevent biofilm formation for certain yeast and bacteria on silicon rubber.[62-64]

The Genus *Variovorax*

Species in the genus *Variovorax* are gram-negative, motile, rod-shaped bacteria from the family *Comamonadaceae* that are found in many diverse locations ranging from the gastrointestinal tract of a zebrafish, drinking water, phenol contaminated soils, and the plant microbiome, and have diverse metabolisms.[65-67] They are known for degrading a variety of toxins and organic compounds.[68-72]

There are nine species of *Variovorax,* including *V. boronicumulans, V. defluvii, V. dokdonensis, V. ginsengisoli, V. gossypii, V. guangziensis, V. humicola, V. paradoxus,* and *V. soli,* of which six species have been sequenced.[66] Several *Variovorax* species are plant growth promoting in a variety of plants, including pea (*Pisum sativum*)[73], *Zea mays* [74], and potato (*Solanum tuberosum*).[75] Characteristics that contribute to their ability to promote plant growth have been described. Several *Variovorax* species have 1-aminocyclepropane-1-carboxylate (ACC) deaminase enzyme activity, a plant growth promoting characteristic that lowers the level of the stress hormone ethylene in the plant.[76-78] The plant phytohormone indole-3-acetic acid (IAA) is produced by *V. boronicumulans* using indole-3-acetonitirile (IAN) as a precursor rather than using the more common precursor tryptophan.[79] *V. paradoxus* has shown to help mitigate drought stress in pea plants by increasing nodulation, seed count, and nitrogen content.[80]

Within the *Populus* microbiome, several *Variovorax* species have been isolated, including the thirteen that are the focus of this project and listed in Table 1.1. Twelve of the thirteen were isolated from the endosphere while one was isolated from the rhizosphere, *Variovorax* sp. YR216. Their genomes range in size from 6.03-8.96mb. In addition, the names of the *Variovorax* strains relates to their location of isolation with strains beginning with YR- and CF- isolated from *P. deltoides* trees in North Carolina and Tennessee, respectively, while strains beginning with OK- or OV- were isolated from trees growing in common gardens in Oregon. Additionally, *Variovorax* sp. OK212 and *Variovorax* sp. OK202 were isolated from the same *P. trichocarpa* tree and *Variovorax* sp. OK605 was isolated from the same common garden. *Variovorax* sp. PDC80 was isolated from a *P. deltoides* tree growing in the greenhouse at Oak Ridge National Laboratory in Oak Ridge, Tennessee. The thirteen *Variovorax* species provide a platform by which to investigate differences in plant-associated behavior and in the production of secondary metabolites, such as biosurfactants. Through this research, we were able to identify the biosynthetic potential of the *Variovorax* species as well as differences in growth with other bacterial strains and in different growth environments. Lastly, we have focused on characterizing biosurfactant molecules that are produced by the *Variovorax* species.

Table 1.1: Thirteen *Variovorax* spp. showing the isolation source, size of the genome (Mb), and the GC content. All of the *Populus*-associated *Variovorax* genomes are draft assemblies that range in size from 6.03 Mb (*Variovorax* sp. CF313) to 8.96 Mb (*Variovorax* sp. PDC80).

Name	Source	Size (Mb)	% GC
Variovorax sp. CF079	P. deltoides endosphere	6.85	67.1
Variovorax sp. CF313	P. deltoides endosphere	6.03	67.0
Variovorax sp. PDC80	P. deltoides endosphere	8.96	66.8
Variovorax sp. YR216	P. deltoides rhizosphere	7.37	69.6
Variovorax sp. YR266	P. deltoides endosphere	7.46	66.2
Variovorax sp. YR634	P. deltoides endosphere	7.16	66.4
Variovorax sp. YR750	P. deltoides endosphere	8.10	67.4
Variovorax sp. OK202	P. trichocarpa endosphere	8.80	68.0
Variovorax sp. OK212	P. trichocarpa endosphere	8.80	68.0
Variovorax sp. OK605	P. trichocarpa endosphere	8.80	68.1
Variovorax sp. OV084	P. trichocarpa endosphere	7.39	66.3
Variovorax sp. OV329	P. trichocarpa endosphere	6.31	67.8
Variovorax sp. OV700	P. trichocarpa endosphere	6.48	65.7

CHAPTER TWO :
GENOMIC COMPARISONS AND GENERAL CHARACTERISTICS OF THE *VARIOVORAX* SPECIES

Introduction

The thirteen *Variovorax* species were an ideal experimental set for investigating the genomic and experimental diversity of the closely related species that were all isolated from *Populus*. Previous work using *P. fluorescens* from *Populus* for similar analyses resulted in the discovery of metabolic differences between species isolated from the endosphere and rhizosphere.[38] Given that twelve of the *Variovorax* species were isolated from the endosphere, potential diversity between the species was expected to be reduced. We performed experimental analysis to compare the *Variovorax* species. Growth curves using different medias and carbon sources provided a look into potential metabolic differences for the *Variovorax* species. We also utilized pairwise interaction assays to investigate how the *Variovorax* species may affect the growth of other bacterial strains, which could provide initial information of potential differences in secondary metabolite production.

Additionally, we relied on bioinformatic tools to determine genomic differences between the strains. Analyses included phylogenetic distributions, similarity in proteins for the species, COG identifications, and predicted biosynthetic gene clusters. Overall, the work indicates that the *Variovorax* species encode a high level of genomic and metabolic diversity. Despite being isolated from a common host, these analyses indicate that the *Populus*-associated *Variovorax* strains show variations in metabolic potential, in their interactions, and in the diversity and abundance of biosynthetic gene clusters.

Methods

Strains and Growth Conditions

Bacterial strains used throughout the studies were isolated from the roots of either *Populus deltoides* or *Populus trichocarpa* (Table 1.1, Table 2.1). The bacterial strains were grown at 28-30ºC with shaking in either R2A broth (TEKnova, Inc.), Luria Broth (LB) media (10 g Tryptone, 5 g Yeast Extract, 10 g NaCl per 1 liter), or MOPS minimal media[81] with 10 mM of varying carbon sources (galactose, mannose, malate, sodium acetate, glucose, and sodium citrate).

Genome-wide ANI Analysis

A similarity matrix of genome similarities was calculated using Genome-wide Average Nucleotide Identity (gANI) V1.[82] The dissimilarity matrix was calculated for all pairs and bioNJ[83] was used to create the tree. Both were prepared by Miriam Land from Oak Ridge National Laboratory for analysis.

Growth Curves

The *Variovorax* strains were grown overnight in either R2A or LB media as described previously. The next day, a 96-well microtiter plate was filled with 200 µL of media that the overnight strains were grown in and inoculated with 2 µL of overnight culture. The strains were randomized across the plate to overcome the inaccuracies that may arise due to differences in oxygen flow across the plate and were incubated with the microtiter plate lid. A plate reader (Biotek Synergy 2) was used to automize the readings. The program allowed for automatic reads in addition to applying shaking to the plate between reads.

Table 2.1: List of the 10-member constructed community bacterial strains used for pairwise interaction assay showing the isolation source, size of the genome (Mb), and the GC content.

Genome Name	Isolation Source	Size (Mb)	GC%
Streptomyces YR139	*P. deltoides*	11.45	70.28
Bacillus BC15	*P. deltoides*	5.74	34.79
Caulobacter AP07	*P. deltoides*	5.65	68.89
Rhizobium CF142	*P. deltoides*	7.46	60.15
Sphingobium AP49	*P. deltoides*	4.63	63.19
Burkholderia BT03	*P. deltoides*	10.9	61.88
Duganella CF402	*P. deltoides*	6.24	62.92
Variovorax CF313	*P. deltoides*	6.05	66.80
Pantoea YR343	*P. deltoides*	5.32	54.52
Pseudomonas GM17	*P. deltoides*	6.79	62.79

Growth on Different Carbon Sources

For these experiments, six different carbon sources were tested (galactose, mannose, malate, sodium acetate, glucose, and sodium citrate) with six *Variovorax* strains (*Variovorax* sp. PDC80, *Variovorax* sp. YR216, *Variovorax* sp. YR266, *Variovorax* sp. CF313, *Variovorax* sp. OV700, *Variovorax* sp. YR750). After inoculating, the cultures were incubated at 30ºC with shaking for two days. The optical density (OD) of the cultures was determined at a 600 nm wavelength once every 24 hours.

Pairwise Interaction Assays

Bacterial strains were grown as previously described. R2A plates were prepared with one bacterial strain spread as a lawn on the plate, allowed to dry, then the *Variovorax* strains were spotted on top of the lawn and allowed to dry again. Prepared plates were placed in the incubator at 28ºC for 48 hours. Once grown, the plates were analyzed to determine if the bacterial species had a nuetral, positive, or negative interaction with each other. If neutral, the bacterial spot colony grew normally where it was placed and had no effect on the bacterial lawn. If positive, the bacterial spot colony grew to be larger than where it was placed and had no effect on the bacterial lawn. If negative, the bacterial spot colony produced a halo of no bacterial growth around the colony, demonstrating growth inhibition of the bacterial lawn.

Natural Product Predictions

Accession numbers for the genomes were accessed from the NCBI database and submitted to antiSMASH 4.0 for analysis.[84]

Results

Comparisons of Sequenced Variovorax Genomes

The relative taxonomic positions of the *Populus*-associated genomes were compared using a whole genome Average Nucleotide Identity (ANI) comparison (Figure 2.1).[82] Not surprisingly, the analysis indicates that the six *Variovorax* strains isolated from US water treatment facilities (*V. paradoxus* strains H061 through H112) are highly related as are the four strains isolated from switchgrass roots (NFACC26 through NFACC29). Conversely, the *Populus*-associated genomes are more diverse within the genus and some of the *Populus*-associated genomes occupy niches not covered by other sequenced genomes. The diversity of the *Populus*-associated isolates may reflect, at least in part, different sampling environments based on geographic locations and seasons. Interestingly, three of the strains *Variovorax* sp. YR266, *Variovorax* sp. YR634, and *Variovorax* sp. OV084, are closely related, even though they were isolated from *P. deltoides* in North Carolina and *P. trichocarpa* in Oregon, respectively. Based on this phylogenetic tree, there is little correlation between *Variovorax* strains isolated from *P. deltoides* or *P. trichocarpa* (Table 1.1, Figure 2.1). The exceptions are the closely related strains *Variovorax* sp. OK202 and *Variovorax* sp. OK212 which were isolated from the same *P. trichocarpa* tree and *Variovorax* sp. OK605 isolated from a different *P. trichocarpa* tree growing in the same common garden in Claskanie, Oregon.

Protein Similarity and Orthologs

To begin to look at functional diversity, we constructed a protein similarity half matrix[85]. This matrix shows each pairwise proteome comparison using BLAST to determine whether proteins are shared between the genomes. Proteins that show at least 50% identity over at least 50% of the longest gene product are considered to be in the same family in this analysis (Figure 2.2). Consistent with results from whole genome average nucleotide identity (Figure

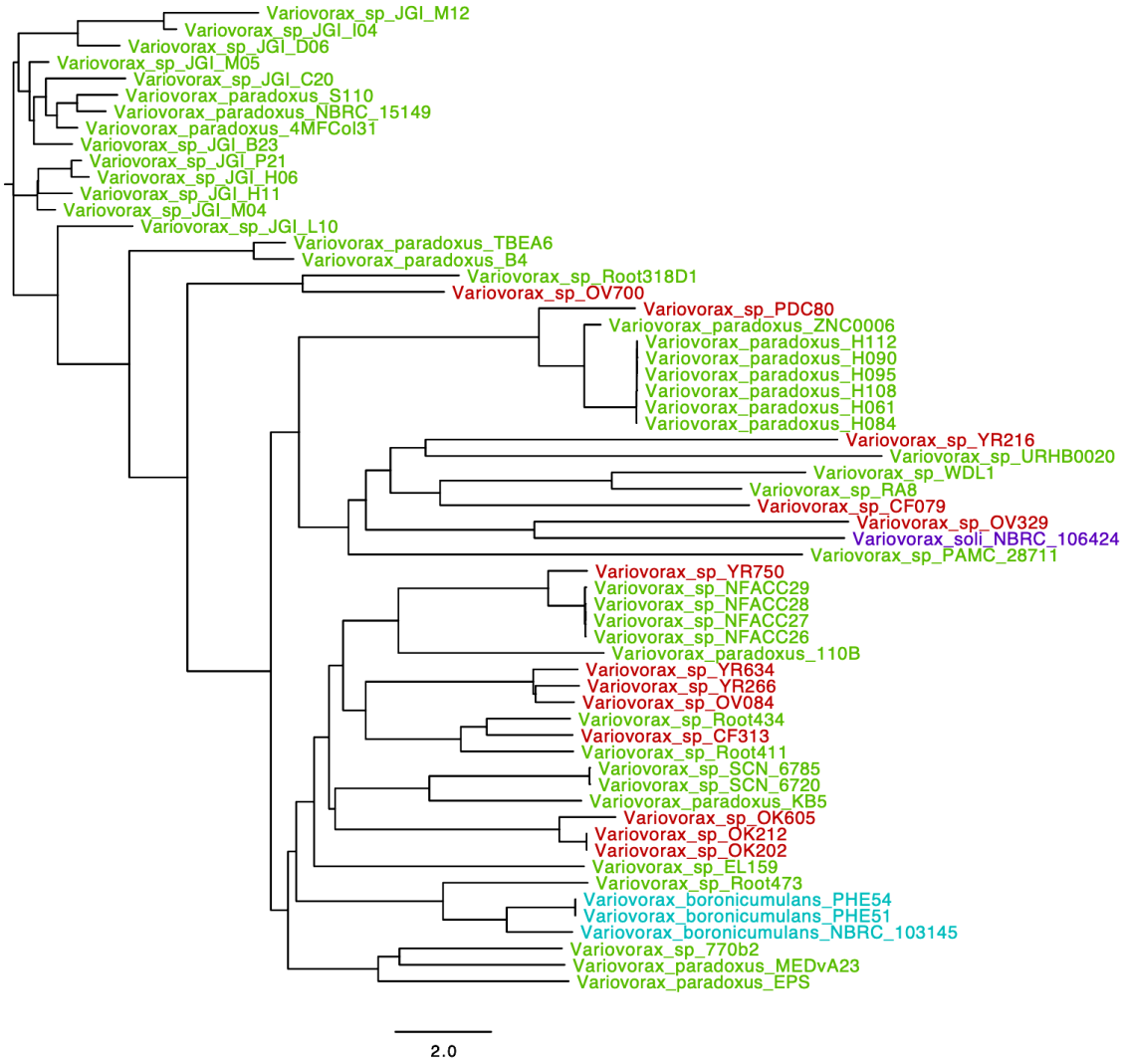

Figure 2.1: Phylogenetic tree for the thirteen *Variovorax* strains using average nucleotide identity (ANI) comparisons, shown in red. The *Variovorax* species highlighted in green, blue, and purple are other sequenced species from the genus. From the ANI comparisons, we found that the *Variovorax* spp. contain two clusters of closely related species.

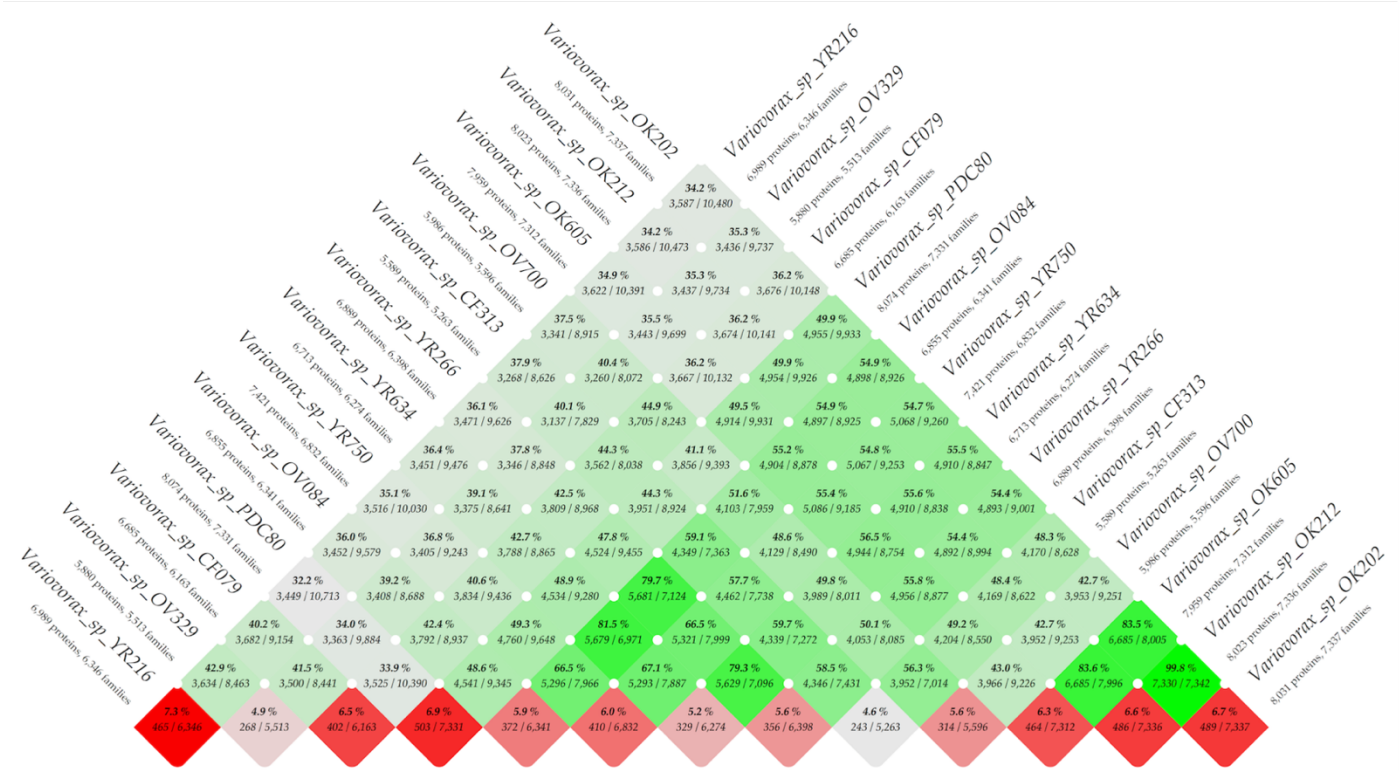

Figure 2.2: A protein similarity half matrix to determine similarities and differences between the proteomes of the *Variovorax* species. The green diamonds represent average percent protein similarity between two genomes (Range: 32.2% -99.8%). The red diamonds are the percent protein similarity within a singular genome (Range: 4.6% -7.3%). The darker the shade of green or red, the more similar the proteome.

2.1), this analysis indicates that *Variovorax* sp. OK605, *Variovorax* sp. OK212, and *Variovorax* sp. OK202 are closely related, showing between 83-99% similarity at the protein level (Figure 2.2). Likewise, *Variovorax* sp. YR634, *Variovorax* sp. YR266, and *Variovorax* sp. OV084 are also closely related, showing between 79-81% protein similarity. Interestingly, *Variovorax* sp. YR216, which was the only strain isolated from the rhizosphere, is the least similar to the other *Populus*-associated strains, ranging from 32-42% similarity at the protein level.

Signaling Pathways

Many bacteria utilize quorum sensing signals to regulate cell-density dependent processes and interactions with hosts.[86] Previous analysis of the *Populus* microbiome showed a prevalence of LuxI- and LuxR- type quorum sensing systems in *Proteobacteria* isolated from the rhizosphere and endosphere of these trees.[87] Thus, we looked for the presence of predicted LuxI/LuxR pairs in the *Variovorax* isolates, using COG3916 to define predicted LuxI homologs and Pfam03472 to define predicted LuxR homologs (Table 2.2). This analysis indicated that six of the isolates (*Variovorax* sp. CF079, *Variovorax* sp. OK202, *Variovorax* sp. OK212, *Variovorax* sp. OK605, *Variovorax* sp. YR266, and *Variovorax* sp. YR750) had well-defined LuxI-LuxR pairs as determined by homology and close proximity in the genome. Another five isolates (*Variovorax* sp. CF079, *Variovorax* sp. CF313, *Variovorax* sp. PDC80, *Variovorax* sp. OV700, and *Variovorax* sp. YR750) encode for orphan LuxR homologs, which may recognize signals produced by other organisms.[88] Only *Variovorax* sp. OV084 and *Variovorax* sp. YR216 showed no apparent LuxI-LuxR signaling systems.

Interestingly, *Variovorax* is also known for the ability to degrade acyl-homoserine lactones (AHL) and disrupt quorum signaling.[67] The main enzymes that confer the ability to degrade AHLs are lactonases and AHL acylases.

Table 2.2: Comparisons of COG and select Pfam families for the *Variovorax* species. The number of genes per COG or Pfam family are listed for each *Variovorax* species as well as the functional category and description for each COG or Pfam.

Functional Category	Description	COG/Pfam	CF079	CF313	PDC80	OK202	OK212	OK605	OV084	OV329	OV700	YR216	YR266	YR634	YR750
Signaling	GGDEF domain, diguanylate cyclase (c-di-GMP synthetase)	COG2199	2	5	8	13	13	13	6	0	4	0	6	6	8
	EAL domain, c-di-GMP-specific phosphodiesterase class I	COG2200	2	2	5	2	2	2	1	0	1	0	1	1	4
	c-di-GMP-related signal transduction protein, contains EAL and HDOD domains	COG3434	1	0	0	1	1	1	1	1	0	2	1	1	1
	Response regulator c-di-GMP phosphodiesterase, RpfG family, contains REC and HD-GYP domains	COG3437	0	0	0	1	1	1	0	0	0	0	0	0	0

Table 2.2: Continued

Functional Category	Description	COG/Pfam	CF079	CF313	PDC80	OK202	OK212	OK605	OV084	OV329	OV700	YR216	YR266	YR634	YR750
	Predicted signal transduction protein containing a membrane domain, an EAL and a GGDEF domain	COG5001	0	1	2	3	3	3	2	0	1	0	1	1	1
	N-acyl-L-homoserine lactone synthetase	COG3916	1	0	0	1	1	1	0	1	0	0	1	1	1
	Autoinducer binding domain	Pfam03472	2	1	1	1	1	1	0	1	2	0	1	1	2
	Acyl-homoserine lactone (AHL) acylase PvdQ	COG2366	1	1	7	4	4	4	3	1	0	0	3	3	4
	Glyoxylase or a related metal-dependent hydrolase, beta-lactamase superfamily II [General function prediction only]	COG0491	15	9	9	10	10	8	10	7	12	9	8	10	11
	Metallo-beta-lactamase superfamily	Pfam00753	14	13	13	12	12	12	14	12	14	13	12	15	20

Table 2.2: Continued

Functional Category	Description	COG/Pfam	CF079	CF313	PDC80	OK202	OK212	OK605	OV084	OV329	OV700	YR216	YR266	YR634	YR750
Iron Uptake	TonB receptor	COG0810	1	0	3	2	2	2	0	0	2	1	1	0	1
	iron complex outermembrane recepter protein	COG4773	4	3	18	11	11	10	7	1	5	0	7	7	0
	iron complex outermembrane recepter protein	COG1629	3	4	11	8	8	10	4	3	4	3	4	4	5
	Outer membrane receptor for monomeric catechols	COG4774	2	2	9	6	6	7	3	3	2	2	3	3	5
Motility	Flagellar biosynthesis/type III secretory pathway ATPase	COG1157	2	2	2	2	2	2	1	1	2	1	1	1	2
	Flagellar hook-associated protein FlgK	COG1256	1	0	1	1	1	1	1	1	0	1	1	1	1
	Flagella basal body P-ring formation protein FlgA	COG1261	1	0	2	1	1	1	1	1	0	1	1	1	1
	Flagellar motor component MotA	COG1291	1	0	1	1	1	1	1	1	0	1	1	1	1

Table 2.2: Continued

Functional Category	Description	COG/Pfam	CF079	CF313	PDC80	OK202	OK212	OK605	OV084	OV329	OV700	YR216	YR266	YR634	YR750
	Flagellar biosynthesis pathway, component FlhA	COG1298	1	1	2	1	1	1	1	1	1	1	1	1	1
	Flagellar biosynthesis/type III secretory pathway protein FliH	COG1317	2	2	2	2	2	2	1	1	2	1	1	1	2
	Flagellar biosynthetic protein FliP	COG1338	1	1	2	1	1	1	1	1	1	1	1	1	1
	Flagellin and related hook-associated protein FlgL	COG1344	2	0	2	2	2	2	2	2	0	2	2	2	2
	Flagellar capping protein FliD	COG1345	1	0	1	1	1	1	1	1	0	1	1	1	1
	Flagellar motor protein MotB	COG1360	1	0	1	1	1	1	1	2	0	1	1	1	1
	Flagellar biosynthesis protein FlhB	COG1377	2	2	2	1	1	1	1	1	2	1	1	1	2
	Flagellar biosynthesis GTPase FlhF	COG1419	1	0	1	1	1	1	1	1	0	1	1	1	1

Table 2.2: Continued

Functional Category	Description	COG/Pfam	CF079	CF313	PDC80	OK202	OK212	OK605	OV084	OV329	OV700	YR216	YR266	YR634	YR750
	Flagellin-specific chaperone FliS	COG1516	1	0	1	1	1	1	1	1	0	1	1	1	1
	Flagellar motor switch protein FliG	COG1536	1	0	1	1	1	1	1	1	0	1	1	1	1
	Flagellar basal body rod protein FlgC	COG1558	1	1	2	1	1	1	1	1	1	1	1	1	1
	Flagellar basal body-associated protein FliL	COG1580	2	0	1	1	1	1	1	1	0	1	1	1	1
	Flagellar hook-basal body complex protein FliE	COG1677	1	1	2	1	1	1	1	1	1	1	1	1	1
	Flagellar biosynthesis protein FliR	COG1684	1	1	2	1	1	1	1	1	1	1	1	1	1
	Flagellum-specific peptidoglycan hydrolase FlgJ	COG1705	1	0	1	1	1	1	1	1	0	1	1	1	1
	Flagellar basal body P-ring protein FlgI	COG1706	1	1	2	1	1	1	1	1	1	1	1	1	1
	Flagellar hook protein FlgE	COG1749	1	1	2	1	1	1	1	1	1	1	1	1	1

Table 2.2: Continued

Functional Category	Description	COG/Pfam	CF079	CF313	PDC80	OK202	OK212	OK605	OV084	OV329	OV700	YR216	YR266	YR634	YR750
	Flagellar biosynthesis/type III secretory pathway M-ring protein FliF/YscJ	COG1766	1	1	2	1	1	1	1	1	1	1	1	1	1
	Flagellar basal body rod protein FlgB	COG1815	1	1	2	1	1	1	1	1	1	1	1	1	1
	Flagellar hook assembly protein FlgD	COG1843	1	0	1	1	1	1	1	1	0	1	1	1	1
	Flagellar motor switch protein FliM	COG1868	1	0	1	1	1	1	1	1	0	1	1	1	1
	Flagellar motor switch/type III secretory pathway protein FliN	COG1886	1	0	1	1	1	2	1	1	1	1	1	1	1
	Flagellar biosynthesis protein FliQ	COG1987	1	1	2	1	1	1	1	1	1	1	1	1	1
	Flagellar basal body L-ring protein FlgH	COG2063	1	1	2	1	1	1	1	1	1	1	1	1	1
	Flagellar biosynthesis chaperone FliJ	COG2882	1	0	1	1	1	1	1	1	0	1	1	1	1

Table 2.2: Continued

Functional Category	Description	COG/Pfam	CF079	CF313	PDC80	OK202	OK212	OK605	OV084	OV329	OV700	YR216	YR266	YR634	YR750
Chemotaxis	Chemotaxis protein histidine kinase CheA (gene: chemosensory pili system protein ChpA (sensor histidine kinase/response regulator))	COG0643	2	1	1	2	2	2	2	2	1	2	2	2	2
	twitching motility two-component system response regulator PilG	Pfam00072	81	79	106	118	118	119	101	88	82	96	102	102	104
	twitching motility two-component system response regulator PilH	Pfam00072	81	79	106	118	118	119	101	88	82	96	102	102	104
	twitching motility protein PilI	COG0835	2	1	1	1	1	3	3	2	3	3	3	3	3
	twitching motility protein PilJ	COG0840	7	1	1	16	16	17	8	11	2	12	8	8	14
	Methyl-accepting chemotaxis proteins	Pfam00015	7	1	1	16	16	17	8	11	2	12	8	8	14

Putative lactonases were searched using COG0491 and Pfam00753 and were found in all of the *Variovorax* strains (Table 2.2). Putative AHL acylases were searched using COG2366 or Pfam01804 and were found in all strains except *Variovorax* sp. YR216 and *Variovorax* sp. OV700 (Table 2.2).

Chemotaxis

Using comparative genomic analysis, we examined the chemotaxis operons present in each of the 13 *Variovorax* species used throughout this study. We found that all of the *Variovorax* species contain an operon for the Chp chemosensory pathway which has been shown in other species to regulate the production and function of type IV pili and twitching motility.[89,90] All of the Chp chemosensory pathways included *pilHIJ* and *chpA*, and variations in this operon across strains included genes encoding rubredoxin (a low molecular weight iron-containing protein involved in electron transfer) in several strains, like *Variovorax* sp. CF313, and others also possessed *pilG* (Table 2.2). In addition to the Chp chemosensory pathway, we found that all of the *Variovorax* strains in this study, except for *Variovorax* sp. CF313 and *Variovorax* sp. PDC80, possessed a separate operon containing chemotaxis genes. The structure of this operon was identical in ten of the *Variovorax* strains and included genes for flagella biosynthesis (*flhD*, *flhC*, *motA*), chemotaxis (*cheA*, *cheB*, *cheY*, *cheZ* and *cheD*), and a gene encoding a putative phosphodiesterase (EAL domain-containing protein). *Variovorax* sp. OV700, on the other hand, contained an operon resembling that of the Wsp system described for *Pseudomonas*, consisting of genes encoding *wspABCDF*, a diguanylate cyclase - response regulator hybrid protein, and phospholipase C.[91] MCPs used to bind chemical signals for chemotaxis also vary in number across the thirteen strains.[8] *Variovorax* sp. CF313 and *Variovorax* sp. PDC80 have the least number of genes with one MCP each, while *Variovorax* sp. OK605 has the most with 17 MCP genes (Table 2.2).

Natural Product Predictions

In order to determine predicted natural products produced by the *Variovorax* species, we utilized antiSMASH 4.0 for predictions and analysis of biosynthetic gene clusters found in their genomes [84]. We found that the *Variovorax* species are predicted to have biosynthetic gene clusters that cover thirteen natural product categories (Table 2.3). The *Variovorax* species are most abundant in predicted nonribosomal peptide synthetase (NRPS) biosynthetic gene clusters (count: 38) and the hybrid Type 1 Polyketide Synthase (T1PKS)-NRPS biosynthetic gene clusters (count: 23). NRPS biosynthetic gene clusters make up a diverse family of metabolites that range in properties including siderophores, biosurfactants, antimicrobials, and toxins.[92] Other *Variovorax* species have predicted biosynthetic gene clusters that are unique to only one species such as *Variovorax* sp. CF079 containing a predicted siderophore cluster, *Variovorax* sp. OV700 containing a predicted hybrid thiopeptide-bacteriocin cluster, and *Variovorax* sp. YR750 containing a predicted TransAT-PKS cluster, further demonstrating the diversity found within the genus. Particular clusters of interest include arylpolyene, which can produce pigments that protect bacteria from reactive oxygen species (ROS) and were recently characterized structurally for *Variovorax paradoxus* B4.[93] Lastly, the *Variovorax* species have predicted terpene biosynthetic gene clusters. Terpenes are small volatile compounds that are suggested to act as intra- and inter-species communication molecules within the soil.[94]

Further analysis of the predicted NRPS clusters resulted in the discovery of a highly conserved gene cluster among the *Variovorax* species. When the gene from *Variovorax* sp. OK202 was used as the template for BLAST, the results for the genes ranged in percent identity from 100% to 48% and all genes were predicted to be a hybrid T1PKS/NRPS gene cluster through antiSMASH (Table 2.4). Additionally, the gene neighborhoods are highly similar (Figure 2.3).

Table 2.3: Results from antiSMASH analysis for the *Variovorax* species. The predicted antiSMASH categories are listed along the top of the table as well as the number of antiSMASH Gene Clusters predicted in each *Variovorax* species.

Genome Name	arylpolyene	arylpolyene-resorcinol	bacteriocin	hserlactone	lantipeptide	nrps	other	resorcinol	siderophore	t1pks-nrps	terpene	thiopeptide-bacteriocin	transatpks	antiSMASH cluster
Variovorax sp. CF079	1		1	1		3	1	1	1	1	1			11
Variovorax sp. CF313	1	1	1			2	1	1		2	1			10
Variovorax sp. OK202	1	1		1	1	5		1		2	1			13
Variovorax sp. OK212	1	1		1	1	5		1		2	1			13
Variovorax sp. OK605	1	1		1	1	3		1		2	1			11
Variovorax sp. OV084	1	1	1			2		1		2	1			9
Variovorax sp. OV329	2		1	1		2				1	1			8
Variovorax sp. OV700	1	1	1					1		3	1	1		9
Variovorax sp. PDC80	1	1				1		1		2	1			7
Variovorax sp. YR216	1		2			1	1			1	1			7
Variovorax sp. YR266	1	1	1	1		7	1	1		2	1			16
Variovorax sp. YR634	1	1	1	1		1		1		2	1			9
Variovorax sp. YR750	1	1	1	1		6		1		3	1		2	17
Total	14	10	10	8	3	38	4	11	1	25	13	1	2	140

Table 2.4: Results for the highly conserved biosynthetic gene cluster found in the *Variovorax* species. BLAST results demonstrate similarities between the *Variovorax* genes compared to the gene found in *Variovorax* sp. OK202. Homologous known gene clusters and NaPDoS results provide predictions of possible products by the biosynthetic gene clusters.

		BLAST Results			Homologous Known Gene Clusters			NaPDoS Results		
Genome	**Cluster Type (#)**	**% ID**	**IMG Locus Tag**	**Gene Name**	**% ID**	**Gene Cluster Name**	**Organism**	**% ID**	**Domain Result**	**Organism**
OK202	T1PKS-NRPS (3)	100	Ga0115515_103445	amino acid adenylation domain-containing protein	14	Colanic Acid	*E. coli*	32	Microcystin	*E. coli*
OK212	T1PKS-NRPS (3)	100	Ga0115516_103445	amino acid adenylation domain-containing protein	14	Colanic Acid	*E. coli*	32	Microcystin	*E. coli*
OK605	T1PKS-NRPS (1)	99	Ga0070142_101292	amino acid adenylation domain-containing protein	9	Colanic Acid	*E. coli*	32	Microcystin	*E. coli*
OV084	T1PKS-NRPS (2)	88	Ga0115518_101859	amino acid adenylation domain-containing protein	9	Colanic Acid	*E. coli*	34	Microcystin	*E. coli*
CF313	T1PKS-NRPS (4)	87	PMI12_02243	amino acid adenylation domain-containing protein	9	Colanic Acid	*E. coli*	35	Microcystin	*E. coli*
YR266	T1PKS-NRPS (1)	88	Ga0115523_102335	amino acid adenylation domain-containing protein	9	Colanic Acid	*E. coli*	34	Microcystin	*E. coli*
YR634	T1PKS-NRPS (8)	88	Ga0115524_12133	amino acid adenylation domain-containing protein	9	Colanic Acid	*E. coli*	34	Microcystin	*E. coli*
YR750	T1PKS-NRPS (1)	86	Ga0115525_101262	amino acid adenylation domain-containing protein	22	Lipopolysaccharide	*E. coli*	32	Microcystin	*E. coli*
OV700	T1PKS-NRPS (6)	75	Ga0115520_105323	amino acid adenylation domain-containing protein	10	Colanic Acid	*E. coli*	34	Microcystin	*E. coli*
PDC80	T1PKS-NRPS (5)	69	Ga0115521_110312	amino acid adenylation domain-containing protein	14	Colanic Acid	*E. coli*	35	Microcystin	*E. coli*

Table 2.4: Continued

		BLAST Results			Homologous Known Gene Clusters			NaPDoS Results		
Genome	**Cluster Type (#)**	**% ID**	**IMG Locus Tag**	**Gene Name**	**% ID**	**Gene Cluster Name**	**Organism**	**% ID**	**Domain Result**	**Organism**
YR216	T1PKS-NRPS (4)	56	Ga0115522_10569	amino acid adenylation domain-containing protein	N/A	N/A	N/A	37	Microcystin	*E. coli*
OV329	T1PKS-NRPS (4)	48	Ga0115519_108217	amino acid adenylation domain-containing protein	N/A	N/A	N/A	34	Microcystin	*E. coli*

Figure 2.3: Gene neighborhood for highly conserved gene cluster found in the *Variovorax* species through antiSMASH. The genes highlighted in red were used for the BLAST and product prediction searches.

Possible products for the biosynthetic gene clusters were investigated using bioinformatic tools through the antiSMASH website. We first looked at predictions from antiSMASH for similarities between the predicted biosynthetic gene clusters to homologous known gene clusters. This suggested nine of the gene clusters could be related to the exopolysaccharide colanic acid.[95] However, there is only a 9-14% match between the *Variovorax* species and a known colanic acid biosynthetic gene cluster from *Escherichia coli* (Table 2.4). Furthermore, one species, *Variovorax* sp. YR750 is not a match for colanic acid but rather has a 22% match to a lipopolysaccharide biosynthetic gene cluster from *E. coli.* Another three, *Variovorax* sp. YR216, *Variovorax* sp. CF079, and *Variovorax* sp. OV329, did not have a match towards any homologous known gene cluster. We next used NaPDoS to further analyze the gene cluster which compares the condensation domains of the predicted genes to known natural product condensation domains.[96] The condensation domains are one of the specific domains in NRPS and hybrid PKS/NRPS gene clusters and are identified through the gene cluster annotation feature in antiSMASH.[84] The domains were found to match from 32-37% for a microcystin domain from *Microcystis aeruginosa,* a highly toxic compound produced by the cyanobacteria (Table 2.4).[97]

Growth Curves in Different Medias

In order to determine growth differences between the *Variovorax* strains, we performed growth curves using LB, a rich media, and R2A, a less rich but not minimal media. The growth curves ran for 24 hours in a standard microtiter plate to be monitored by a plate reader. We found that eight of the thirteen *Variovorax* strains grew well on both R2A and LB: *Variovorax* sp. OV700, *Variovorax* sp. PDC80, *Variovorax* sp. OV329, *Variovorax* sp. YR750, *Variovorax* sp. CF313, *Variovorax* sp. YR634, *Variovorax* sp. YR266, and *Variovorax* sp. OV084 (Figure 2.4, 2.5, 2.6). The remaining five grew with preference to either R2A or LB.

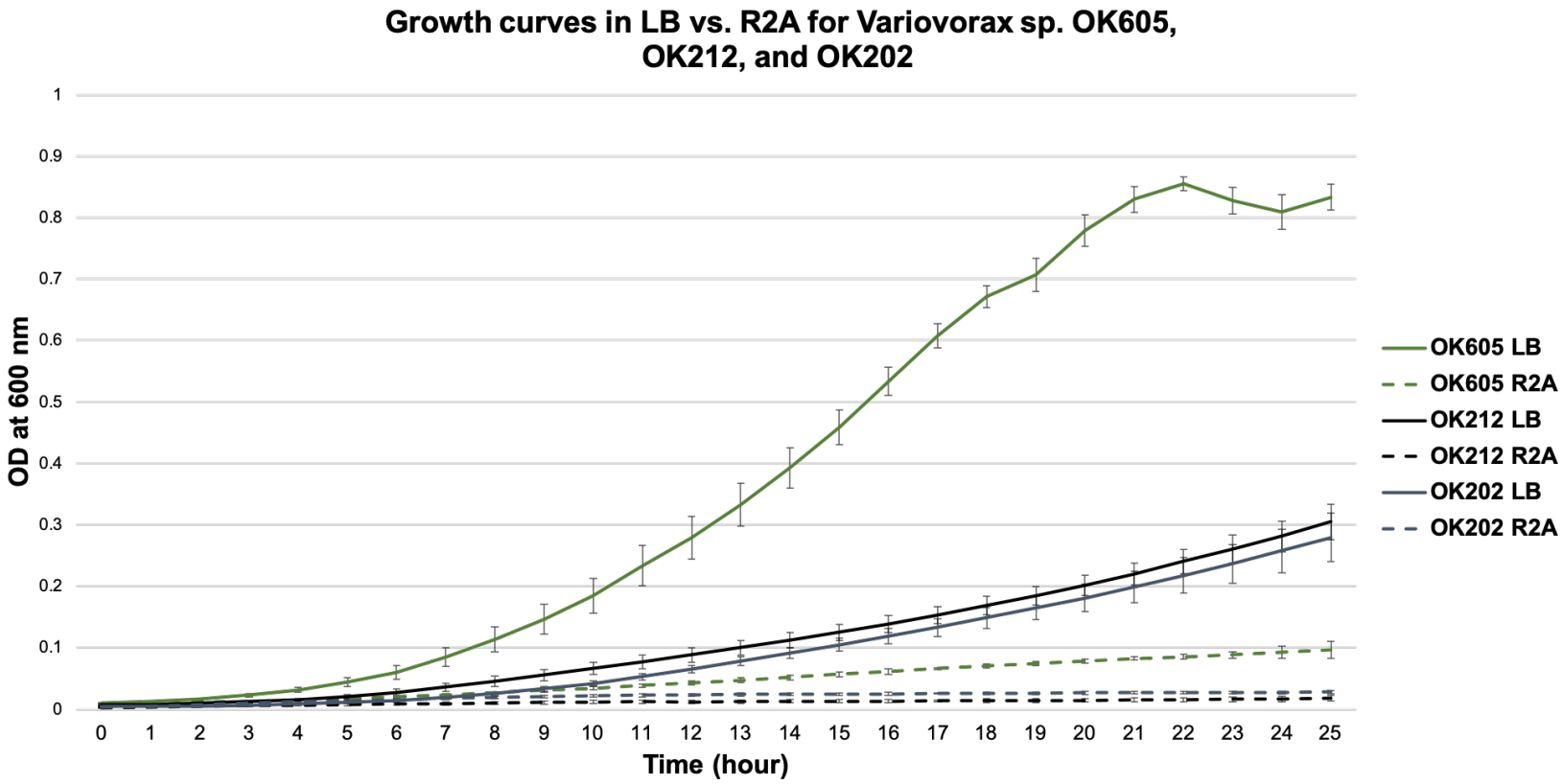

Figure 2.4: Growth curves for phylogenetic clusters containing *Variovorax* sp. OK605, *Variovorax* sp. OK212, and *Variovorax* sp. OK202 in R2A and LB media. The solid lines are growth curves in LB media and the dashed lines are growth curves in R2A media.

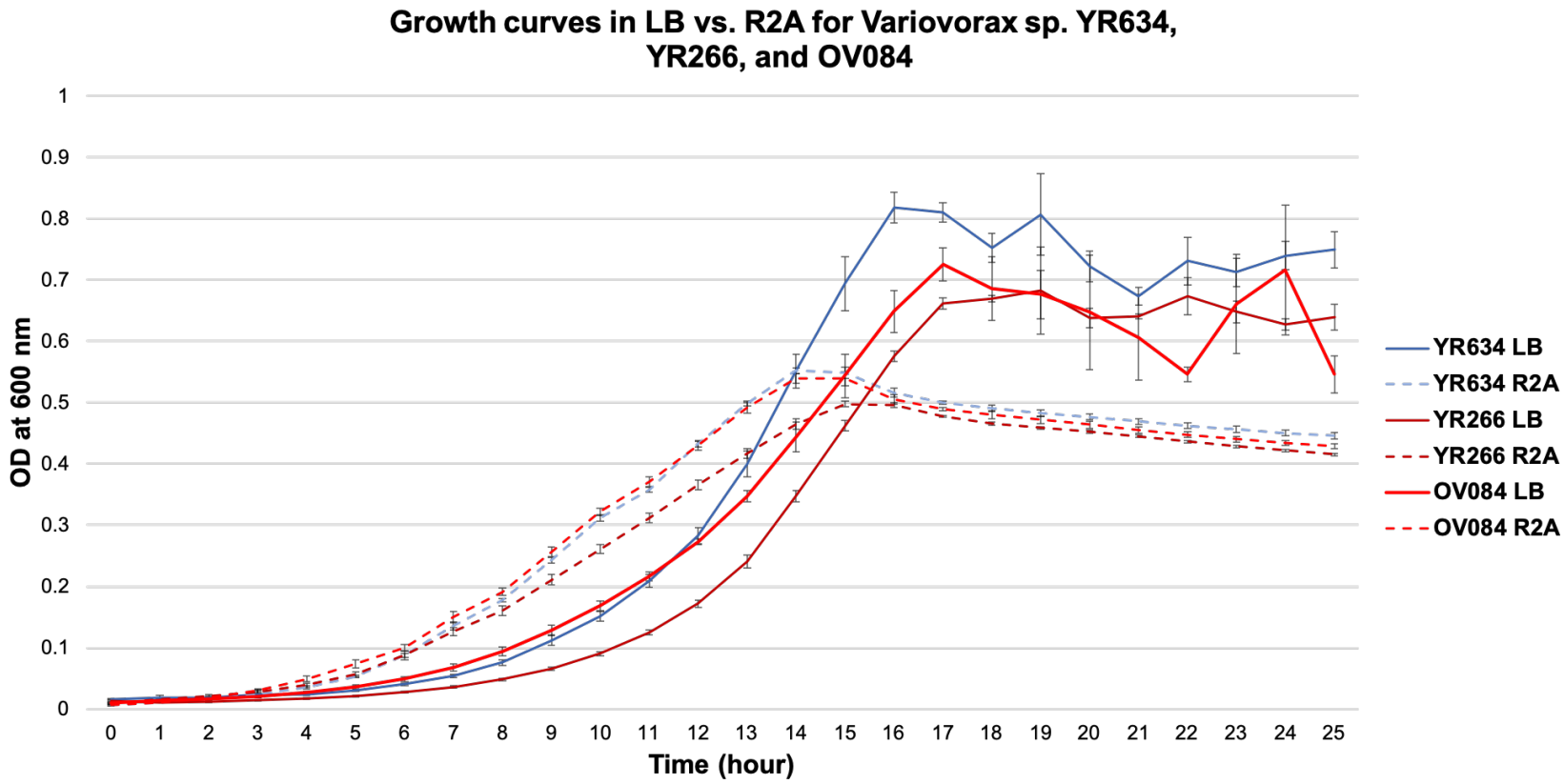

Figure 2.5: Growth curves in R2A and LB media for phylogenetic clusters containing *Variovorax* sp. YR634, *Variovorax* sp. YR266, *Variovorax* sp. OV084. The solid lines are growth curves in LB media and the dashed lines are growth curves in R2A media.

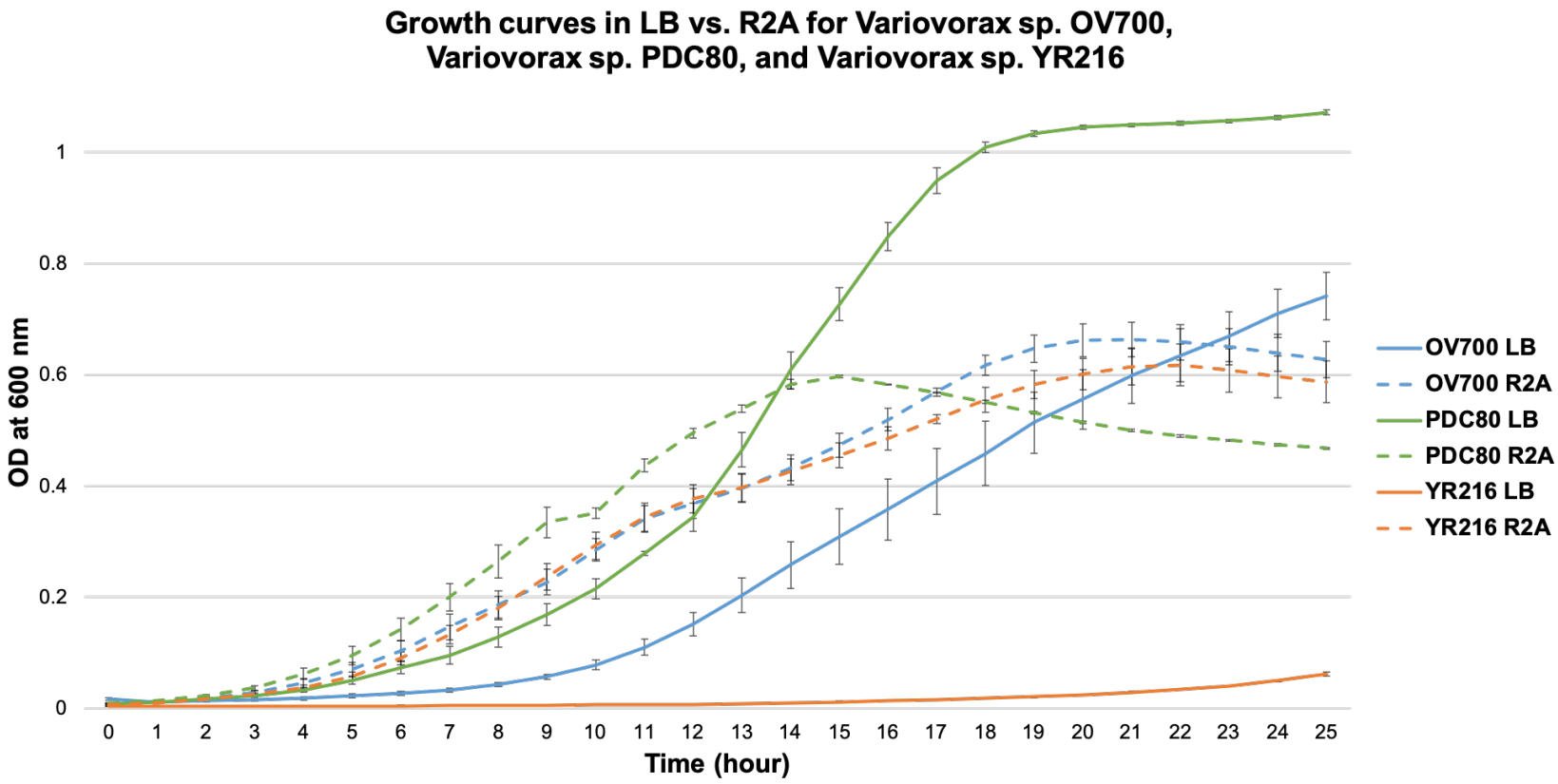

Figure 2.6: Growth curves in R2A and LB media for *Variovorax* sp. OV700, *Variovorax* sp. PDC80, *Variovorax* sp. YR216. The solid lines are growth curves in LB media and the dashed lines are growth curves in R2A media.

Variovorax sp. OK605, *Variovorax* sp. OK212, *Variovorax* sp. OK202 grew better in LB while *Variovorax* sp. YR216 and *Variovorax* sp. CF079 preferred R2A (Figure 2.4, 2.6, 2.7). The bacterial strains with preference to one or the other appear to have longer lag times in certain medias than others. The doubling times for the *Variovorax* species are listed in Table 2.5.

We also analyzed the growth curves based on the phylogenetically similar clusters for the *Variovorax* strains to determine if the strains demonstrate similar growth patterns. The cluster containing *Variovorax* sp. OK605, *Variovorax* sp. OK202, and *Variovorax* sp. OK212 demonstrated *Variovorax* sp. OK605 grew significantly better than *Variovorax* sp. OK202 and *Variovorax* sp. OK212 in both LB and R2A, suggesting metabolic differences between these closely similar species (Figure 2.4). All three also demonstrated similar growth media preferences with each species growing better in LB rather than R2A. The second cluster containing *Variovorax* sp. YR634, *Variovorax* sp. YR266, and *Variovorax* sp. OV084 grew similarly to each other in both R2A and LB with their highest ODs being significantly higher in LB (0.66- 0.82) than in R2A (0.49- 0.54) (Figure 2.5).

Next, to further investigate their metabolic diversity, we used six different carbon sources (galactose, mannose, malate, sodium acetate, glucose, and sodium citrate) with six *Variovorax* strains (*Variovorax* sp. PDC80, *Variovorax* sp. YR216, *Variovorax* sp. YR266, *Variovorax* sp. CF313, *Variovorax* sp. OV700, *Variovorax* sp. YR750), as shown in Figure 2.8. The data indicated that four of the six strains (*Variovorax* sp. YR266, *Variovorax* sp. CF313, *Variovorax* sp. YR750, *Variovorax* sp. OV700) grew well with galactose as the carbon source, with an OD range of 0.262-0.379. *Variovorax* sp. YR750 and *Variovorax* sp. PDC80 grew best using glucose (the OD for each being 0.369 and 0.244, respectively). Interestingly, *Variovorax* sp. YR750 grew equally well in MOPS with glucose, MOPS with galactose, and MOPS with mannose. All other strains

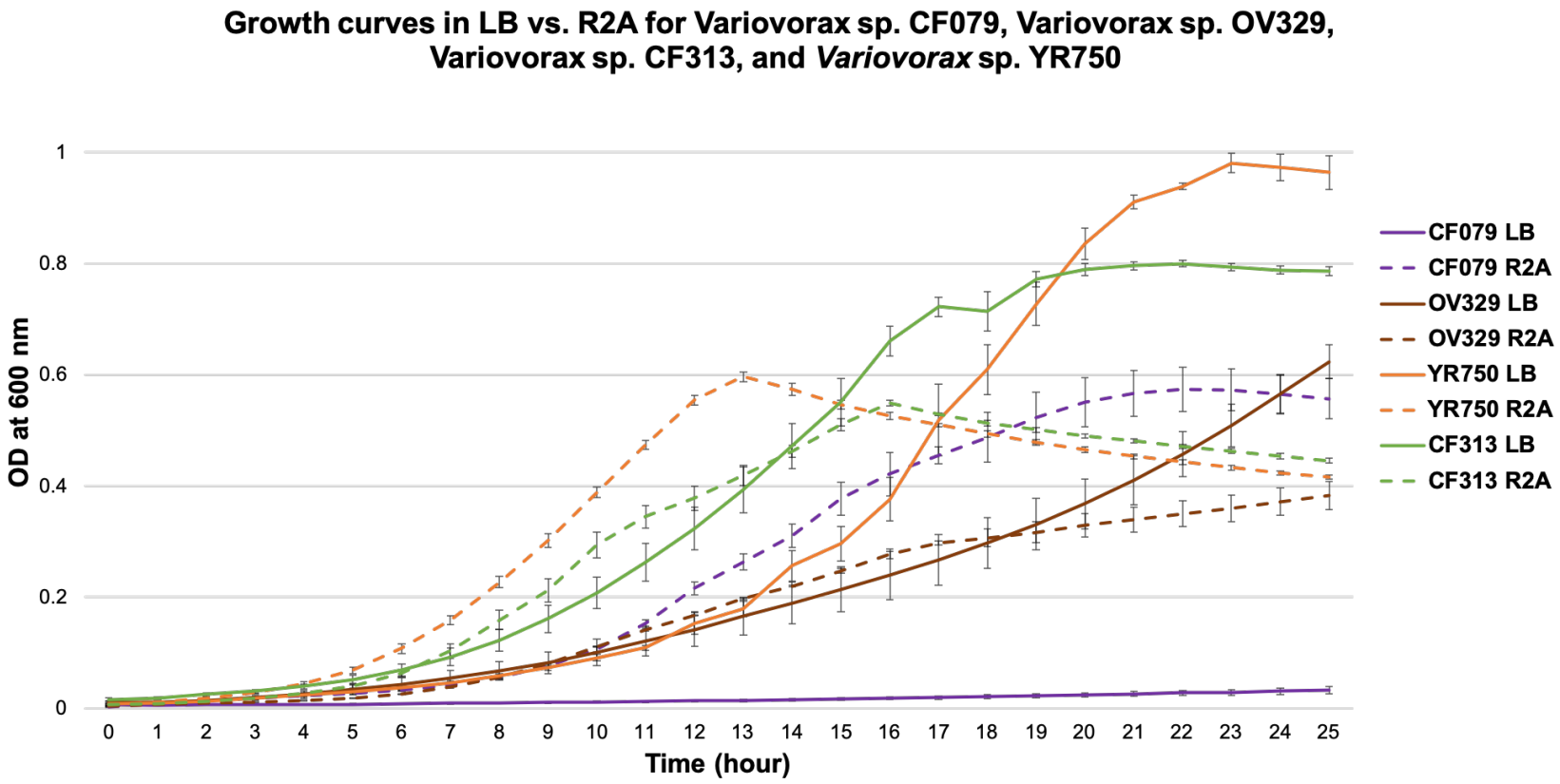

Figure 2.7: Growth curves in R2A and LB media for *Variovorax* sp. CF079, *Variovorax* sp. OV329, *Variovorax* sp. YR750, and *Variovorax* sp. CF313. The solid lines are growth curves in LB media and the dashed lines are growth curves in R2A media.

Table 2.5: Doubling times for the *Variovorax* species using the growth curves in LB and R2A media for analysis.

Species	Doubling time in LB (hours)	Doubling time in R2A (hours)
Variovorax sp. CF079	10.0	3.0
Variovorax sp. CF313	3.3	3.7
Variovorax sp. OK202	7.3	17.3
Variovorax sp. OK212	7.9	17.0
Variovorax sp. OK605	3.2	11.1
Variovorax sp. OV084	3.5	3.3
Variovorax sp. OV329	6.6	3.1
Variovorax sp. OV700	4.6	4.7
Variovorax sp. PDC80	3.2	3.6
Variovorax sp. YR216	3.7	4.0
Variovorax sp. YR266	2.7	4.3
Variovorax sp. YR634	2.6	3.0
Variovorax sp. YR750	3.3	2.8

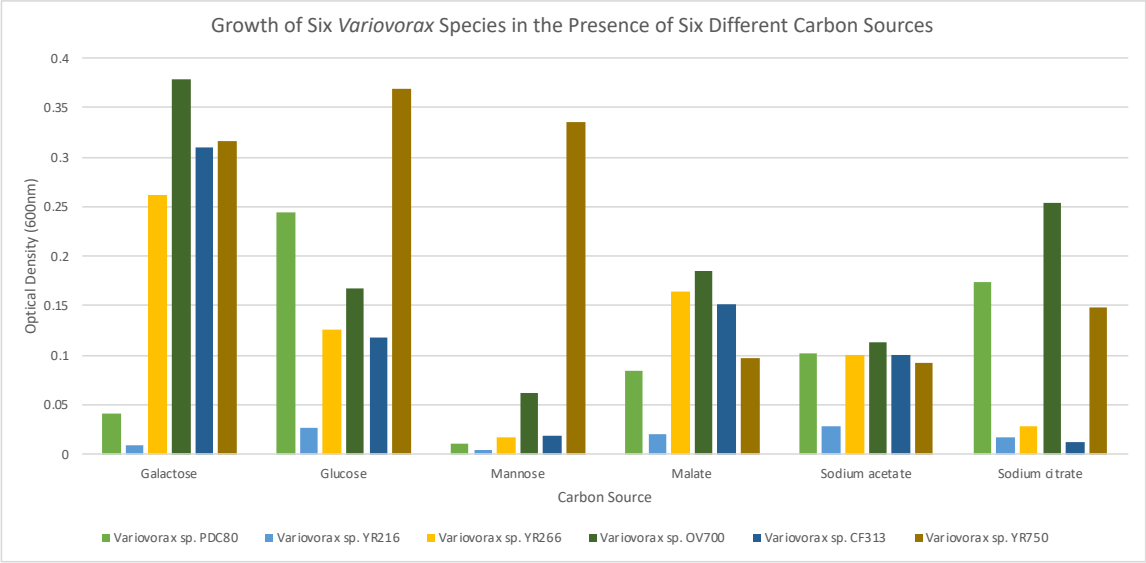

Figure 2.8: Growth assay for six *Variovorax* species in MOPS minimal media using six different carbon sources at a 10 mM concentration.

demonstrated a clear preference for only one of the carbon sources where the best carbon source produced an OD that was 0.1-0.2 higher than the other carbon ODs. Finally, *Variovorax* sp. YR216 grew the least in all the carbon sources, with its OD reaching its highest at 0.071 in MOPS with glucose added, much lower than any of the other strains. Genomic analysis for Phosphotransferase Systems (PTS) determined that all of the *Variovorax* species encode four to eight transporters with a range of two to four being sugar specific PTS systems. *Variovorax* sp. CF313 has the most with four general PTS and four sugar specific PTS transporters. *Variovorax* sp. YR266 have two general PTS and three sugar specific PTS transporters. The remaining four, *Variovorax* sp. YR750, *Variovorax* sp. OV700, *Variovorax* sp. PDC80, and *Variovorax* sp. YR216, each have two general PTS and two sugar specific PTS transporters. These differences in growth suggest metabolic differences between the *Variovorax* species which in turn could lead to differences within the microbiome and colonization based on the root exudate profile of the plant.

Pairwise Interaction Data

Pairwise interaction assays were then used to look at how one bacterial isolate affects the growth of another to answer the question of whether the *Variovorax* species can influence of the growth of other *Populus* isolates. To conduct the assays, a bacterial species was spread as a lawn on R2A medium. Then, other bacterial species were spotted on the top of the bacterial lawn and placed in a 28ºC incubator for 1-2 days depending on how quickly the bacterial strains grew. Once grown, the plates were analyzed to determine if the bacterial species had a nuetral, positive, or negative interaction with each other. If neutral, the bacterial spot colony grew normally and had no effect on the bacterial lawn. If positive, the bacterial spot colony had enhanced growth and no effect on the bacterial lawn. If negative, the bacterial spot colony inhibited the growth of the bacterial lawn, producing a halo around the colony.

The first pairwise interaction assay utilized a 10-member community of *Populus* isolates as the bacterial lawn species with the 13 *Variovorax* species as the bacterial spots. The 10-member community was previously created as a representative sample of the *Populus* microbiome but were not picked due to an anticipated interaction with the *Variovorax* strains. A total of three experiments were conducted and an average of the results are shown in Figure 2.9. From these assays, it is concluded that the *Variovorax* species have the ability to inhibit growth of several bacterial species, such as *Variovorax* sp. PDC80 having negative interactions on five different bacterial species. This suggests that the *Variovorax* species may compete for nutrients or space with the bacterial strain in the lawn or that the *Variovorax* sp. PDC80 may be producing a compound with antimicrobial activity that is specific to certain bacterial species. Differences in growth may also play a role in the interactions seen, as suggested by their doubling times (Table 2.5 and 2.6). It is also of interest to note that several of the *Variovorax* species, *Variovorax* sp. YR634, *Variovorax* sp. YR750, *Variovorax* sp. YR266, *Variovorax* sp. OV084, and *Variovorax* sp. OK605, demonstrated a negative interaction on *Variovorax* sp. CF313 when used as the bacterial lawn, suggesting some of the *Variovorax* species can potentially influence the growth of other *Variovorax* genus members.

In order to further investigate possible effects that the *Variovorax* species may have against each other, additional pairwise interaction assays were performed. For this experiment, the same 13 *Variovorax* species were used as the bacterial lawns and the bacterial spots. A total of four experiments were conducted with the average results seen in Figure 2.10. From this experiment, the overall conclusion is that the *Variovorax* species have substantial effects of other members of the genus depending on the interaction involved.

The pairwise interaction assays also demonstrate how the phylogenetic clusters from Figure 2.1 have similar interactions with the bacterial strains in both of the pairwise interaction assays (Figure 2.9 and 2.10). This suggests that the

Table 2.6: Doubling times for the 10 *Populus* isolates used in the pairwise interaction assay. The times were calculated from growth curves of the *Populus* isolates in R2A.

Species	Doubling Times (hours)
Bacillus BC15	1.2
Burkholderia BT03	4.0
Caulobacter AP07	2.9
Duganella CF402	1.4
Pantoea YR343	1.5
Pseudomonas GM17	1.3
Rhizobium CF142	3.5
Sphingobium AP49	1.9
Streptomyces YR139	1.1
Variovorax CF313	2.7

Colony	Bacterial Lawn: *Streptomyces* YR139	*Bacillus* BC15	*Caulobacter* AP07	*Rhizobium* CF142	*Sphingobium* AP49	*Burkholderia* BT03	*Duganella* CF402	*Variovorax* CF313	*Pantoea* YR343	*Pseudomonas* GM17
Variovorax OV700	N	N	N	N	N	+	N	N	N	N
Variovorax PDC80	-	N	-	N	N	-	-	+	N	-
Variovorax YR216	N	N	N	N	N	+	N	N	N	N
Variovorax CF079	N	N	N	N	N	N	N	N	N	N
Variovorax OV329	N	N	N	N	N	N	N	N	-	N
Variovorax YR750	-	N	+	+	N	+	-	-	-	-
Variovorax YR634	-	N	+	+	-	+	-	-	N	-
Variovorax YR266	-	N	-	N	N	+	+	-	N	-
Variovorax OV084	-	N	-	+	N	+	-	-	N	N
Variovorax CF313	N	N	N	N	N	N	N	S	N	-
Variovorax OK605	N	N	N	N	N	N	N	-	N	N
Variovorax OK212	N	N	N	N	N	N	N	N	N	N
Variovorax OK202	N	N	N	N	N	N	N	N	N	N

Key:	
+	Positive
-	Negative
S	Self
N	None

Figure 2.9: Pairwise interaction assay with a 10-member community as bacterial lawns and *Variovorax* species as bacterial colonies spotted on top of the lawns. Interactions are distinguished as either neutral (none), negative, positive, or self. If neutral, the bacterial spot colony grew normally and had no effect on the bacterial lawn. If positive, the bacterial spot colony had additional growth and no effect on the bacterial lawn. If negative, the bacterial spot colony inhibited the growth of the bacterial lawn, producing a halo around the colony. If self, the lawn and spot colony are the same species so no interaction is expected. A total of three replicates per pairwise interaction were obtained.

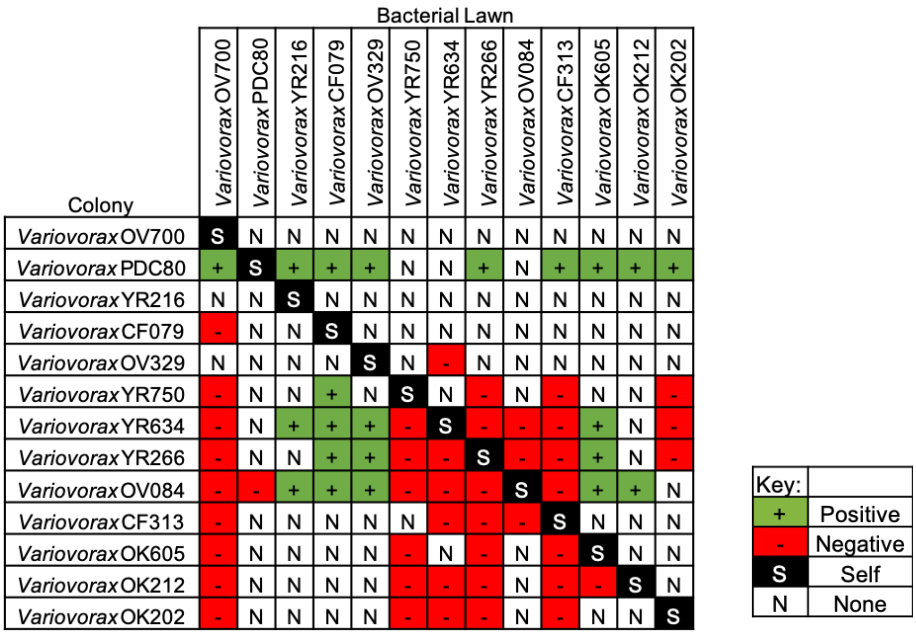

Figure 2.10: Pairwise interaction assay with 13 *Variovorax* species as bacterial lawn and as bacterial colonies spotted on top of the lawns. Interactions are distinguished as either neutral (none), negative, positive, or self. If neutral, the bacterial spot colony grew normally and had no effect on the bacterial lawn. If positive, the bacterial spot colony had additional growth and no effect on the bacterial lawn. If negative, the bacterial spot colony inhibited the growth of the bacterial lawn, producing a halo around the colony. If self, the lawn and spot colony are the same species so no interaction is expected. A total of four replicates per pairwise interaction were obtained.

species within the phylogenetic clusters may have similar natural product makeups or metabolic capabilities which could create similar interactions towards a specific bacterial strain.

Discussion

The phylogenetic analyses of the *Populus*-associated *Variovorax* strains indicate a considerable level of diversity, with some exceptions. For example, *Variovorax* sp. OK202, *Variovorax* sp. OK212, and *Variovorax* sp. OK605 are closely related. Consistent with this, these strains were collected from the same common garden in Claskanie, Oregon in spring 2012, with *Variovorax* sp. OK202 and *Variovorax* sp. OK212 being isolated from roots of the same tree. Likewise, our data shows that *Variovorax* sp. OV084, *Variovorax* sp. YR266, and *Variovorax* sp. YR634 are also closely related. In this case, however, the sampling conditions were much different, with *Variovorax* sp. OV084 being isolated from *P. trichocarpa* in Corvalis, Oregon, and *Variovorax* sp. YR266, and *Variovorax* sp. YR634 being isolated from different *P. deltoides* trees near the Yadkin River in North Carolina in the spring and fall of 2010, respectively.

An additional way for the *Variovorax* strains to influence the *Populus* microbiome is through their ability to use quorum sensing and quenching, which allows for social interactions between bacterial strains through the production of autoinducer proteins when certain cell densities are reached. The AHL signal molecules have also been shown to affect the growth of certain plants directly.[98] The *Variovorax* species that have defined LuxI and LuxR gene pairs could play a role in plant growth promotion through their quorum sensing systems. Orphan LuxR genes are another avenue of interest for how the *Variovorax* species contribute public goods, in the form of natural products, and grow within a microbiome when a strain does not produce its own AHL molecules. It is known that bacteria with orphan LuxRs can respond, by way of gene activation, to small molecules produced by the plant.[99-101] However, it is possible that the bacteria

are perceiving AHLs from other bacteria from their genus.[102] The fact that several of the *Variovorax* strains contain orphan LuxR genes suggests that the strains can perceive the presence of AHLs and respond to them within the microbiome without contributing to the production of the AHLs.

Another role the *Variovorax* strains likely use to influence the microbiome is through their production of natural products. Through our analysis, we have been able to discover many biosynthetic gene clusters within the genomes of the *Variovorax* species. This suggests that the thirteen strains have the ability to produce many natural products, even outside of what we have currently screened. Previous genome mining efforts of *Variovorax boronicumulans* resulted in the discovery of lipopeptide siderophores, demonstrating the ability to translate genome mining predictions to uncovering novel natural products.[103] One important note about the biosynthetic gene clusters is that even with predictions of these clusters, it is possible that the *Variovorax* species do not produce all of the potential products or may only produce a certain product under specific environmental conditions that may not be replicable within a laboratory setting.[43] The antiSMASH predictions for the thirteen *Variovorax* strains suggest that further analysis of the clusters could result in discovery of novel natural products produced within the *Populus* microbiome.

The pairwise interaction assays provide evidence that the *Variovorax* species may be able to affect the growth of other *Populus* isolates within the microbiome. However, one possible explanation for the negative interactions seen in the pairwise interaction assays could be due to nutrient competition between the bacteria as they try to inhabit a singular spot on a plate. Another possibility is that the microbes are producing a compound with antimicrobial properties. If so, these results could lead to future questions of characterizing the antimicrobial compounds and if the results from the pairwise interactions may be transferred to future studies of plant colonization in a more natural environment.

Overall, the results provide preliminary results of the *Variovorax* species influencing the growth of other bacterial species.

This study has resulted in a broad spectrum of analysis for 13 *Variovorax* strains and the roles they may provide to the *Populus* microbiome. In particular, we utilized bioinformatic tools to characterize the phylogenetic distribution of the species, analyze genomic features through COG identifications, and predict natural product potential. Furthermore, we obtained experimental data to investigate potential metabolic differences between the species and determine possible influences the species have on the growth of other bacterial species. Together, we have demonstrated several mechanisms the 13 *Variovorax* strains may use to promote plant growth and provided additional avenues to pursue as we continue to unravel the influence a particular bacterial genus can have within the plant microbiome.

CHAPTER THREE :
BIOSURFACTANT CHARACTERIZATION

Introduction

Characterization of the potential natural products the *Variovorax* species can produce began with looking at potential products from the NRPS clusters. Literature searches for natural products produced from *Variovorax* species led to a few candidates to explore. A lipopeptide siderophore was discovered through genome mining and characterization from *Variovorax boronicumulans* as well as the amphiphilic siderophore, imaqobactin, from *Variovorax* sp. RKJM285. [103,104] Additionally, *Variovorax paradoxus* EPS has been shown to produce a wetting agent which was suggested as a possible biosurfactant.[105] Initial tests for biosurfactant production were positive, leading us to continue characterizing the molecules.

A variety of techniques were used to isolate and begin to characterize the biosurfactants. Crude isolation of the molecules from growing *Variovorax* species were initially used for characterization to determine their ability to reduce surface tension. Analytical techniques allowed for further characterization of the isolated biosurfactant molecules. High performance liquid chromatography (HPLC) provided a way to purify our crude extract which could be used for further characterization. Mass spectrometry imaging (MSI) using Matrix Assisted Laser Desorption/Ionization Time of Flight Mass Spectrometry (MALDI-TOF MS) was used with the goal of verifying that the molecules we extracted were the same molecule that we see on the plate with a growing *Variovorax* colony. These experiments have demonstrated that all thirteen *Variovorax* species produce biosurfactant molecules and that our method development for characterizing these particular molecules is improving for future analysis.

Methods

Strains and Growth Conditions

Thirteen *Variovorax* strains were used throughout the studies (Table 1.1) and were isolated from the roots of either *Populus deltoides* or *Populus trichocarpa*. The bacterial strains were grown at 28-30ºC with shaking in either R2A broth (TEKnova, Inc.), Luria Broth (LB) media (10 g Tryptone, 5 g Yeast Extract, 10 g NaCl per 1 liter), or MOPS minimal media[81] with 10 mM galactose as the carbon source.

Atomized Oil Assay

The descriptive assay was conducted as described.[106] In short, the thirteen *Variovorax* species were spotted on LB plates and allowed to grow for two days. After incubation, the plates were misted with mineral oil using an air spray propellant (Badger Propel). The misted plates were visually analyzed and documented photographically.

Drop Collapse Assay

To determine the ability to collapse drops which is indicative of surfactant properties, a drop collapse assay was used. Water droplets were spotted onto parafilm and then had either the crude biosurfactant extract or the resuspended HPLC-collected fractions were added on top of the water droplet at a ratio of 5:1 of water: biosurfactant sample. The droplets were analyzed immediately and after 5 minutes to determine the collapse of the droplets. The greater the drop collapse, the higher the amount of biosurfactant in the sample.

Crude Biosurfactant Extraction

The biosurfactant molecules were extracted as previously detailed.[107] Briefly, the *Variovorax* strains were grown overnight in R2A to prime the bacteria for biosurfactant production. The next day, a 25 mL R2A culture was inoculated

with 250 µL of the overnight culture and incubated at 30ºC for 96 hours. At that time, the culture was centrifuged at 4ºC at 10,000 g for 10 minutes. The supernatant was filtered through a 0.22 µ Millipore filter under vacuum. The filtered supernatant was acidified to pH 2.0 using HCl and left at 4ºC overnight. The next day, the acidified supernatant was mixed with chloroform-methanol mixture (2:1, v/v), centrifuged at 4ºC at 10,000 g for 20 minutes, and collected the organic phase and discarded the aqueous phase each time. The extraction was performed three times and the organic phase was pooled and dried in a SpeedVac (Thermo Scientific). The resulting material was a viscous, honey to yellow colored material and was stored at -20ºC for further analysis.

Biosurfactant Purification by HPLC Fractionation

The HPLC instrument used (Agilent 1260 Infinity, Agilent Technologies) was equipped with a ZORBAX Eclipse Plus C-18 reversed phase column (4.6 x 100 mm, 3.5µm particle size, Agilent). The initial method was based on Sivapathasekaran, C., Mukherjee, S., Samanta, R. & Sen, R.[108] Solvent A was Milli-Q water and solvent B was acetonitrile (ACN) with 0.1% Trifluoroacetic acid (TFA). The length of the method was 20 minutes, with the first four minutes consisting of a flow rate of 2.00 mL/min with solvent A at 60% and solvent B at 40%. Minutes 4-12 maintained a flow rate of 0.7 mL/min while the solvents fluctuated on a gradient so that solvent A decreased from 40-10% while solvent B increased from 60-90%. The final minutes, from minutes 12-20, the flow rate consisted of 1.00 mL/min and solvent B at 100%. The elution of the peaks was monitored at 210nm. Fractions were collected based on time points and subsequently dried in a SpeedVac. Once dry, fractions were resuspended in 10 µL ethanol.

Our final method maintained the length of the initial method with 20 minutes and the initial four minutes (flow rate of 2.00 mL/min, solvent A at 60%, solvent B at 40%). From minute 4-8, the flow rate increased from 0.7-0.8 mL/min,

solvent A decreased from 40-10%, and solvent B increased from 60-90%. Minute 8-20 consisted of solvent B at 100% and the flow rate increasing from 0.9-1.4 mL/min. The elution of the peaks was monitored at 210nm, initially. Another experiment was performed to monitor elution of the peaks at different wavelengths, using a range of 210-600nm.

Mass Spectrometry Imaging (MSI)

Variovorax sp. YR266 bacterial cultures (spotted as 1 µL overnight culture) were grown on MOPS supplemented with 10 mM galactose on half-sized gold-plated microscope slides. To prevent agar drying while incubating, the samples were placed in a petri dish with damp filter paper. The samples were incubated for two days at 28ºC and dried down using a vacuum desiccator for analysis by Matrix Assisted Laser Desorption/Ionization Time of Flight Mass Spectrometry (MALDI-TOF MS). The samples were placed on a holder that created a flush surface with the MTP slide adapter II (Bruker). The samples were analyzed using a Bruker AutoFlex Max machine in reflective positive mode. The matrix used was 10 mg/mL α-cyano-4-hydroxycinnamic acid (CHCA) dissolved in 50/50/0.1% water/ACN/TFA.

Results

Atomized Oil Assay

To initially determine the production of biosurfactants, we utilized the descriptive atomized oil assay for each of the species.[106] A positive result appeared as a halo of hemispherical oil droplets around the bacteria colony rather than the disordered and distorted oil droplets on a negative plate (Figure 3.1). From the assay, we determined that twelve of the *Variovorax* strains have the phenotype for biosurfactant production. The one negative result was *Variovorax* sp. PDC80 (Table 3.1). However, given the increased motility of

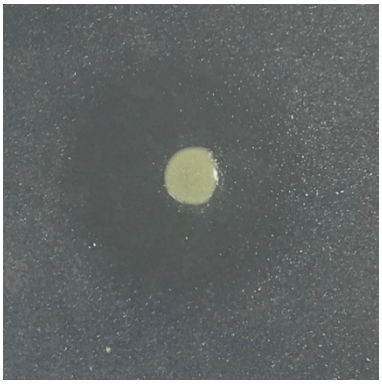

Variovorax sp. OK605

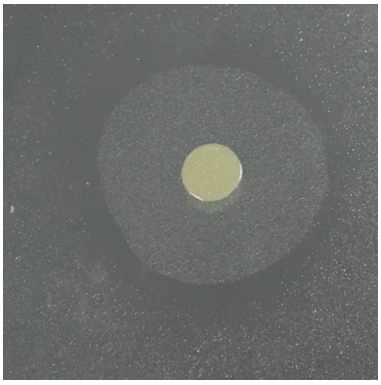

Variovorax sp. YR266

Figure 3.1: Representative results from atomized oil assay in which a positive result is represented by a halo surrounding a growing bacterial strain when misted with mineral oil.

Table 3.1: Results of the atomized oil assay. Twelve of the thirteen strains demonstrated a phenotype of biosurfactant production. An observed halo determined a positive result.

***Variovorax* Species**	**Atomized Oil Assay**
CF079	+
CF313	+
OK202	+
OK212	+
OK605	+
OV084	+
OV329	+
OV700	+
PDC80	-
YR216	+
YR266	+
YR634	+
YR750	+

Variovorax sp. PDC80, its biosurfactant production by the strain may not be evident with this assay and a more quantitative experiment was needed.

Crude Biosurfactant Extraction

To understand the properties of the biosurfactant molecules outside of the *Variovorax* strains that produce them, we sought to extract the molecules from a growing liquid bacterial culture. A chloroform-methanol extraction was utilized for a crude extraction of the biosurfactants and found that the resulting samples have the ability to reduce surface tension, a standard biosurfactant property, as confirmed through drop collapse assays (Figure 3.2). However, the surface tension reduction ability differs depending on the sample. This is likely because the extract is crude and probably contains many components in addition to the biosurfactants.

Biosurfactant Purification by HPLC Fractionation

In order to obtain a purer biosurfactant sample for future characterization and experiments, we utilized HPLC in order to collect fractions and determine which portion of the sample contained biosurfactant activity by measuring the drop collapse ability of each fraction. We initially used a method based on a paper that characterized lipopeptide isoforms from *Bacillus circulans DMS-2.*[108] As a control, we utilized commercially available *B. subtilis* surfactin. Fractions were collected for surfactin and the thirteen *Variovorax* strains. This method proved to work well as the large peaks for surfactin were associated with biosurfactant activity (Figure 3.3). However, with *Variovorax* sp. YR266 the fraction with the highest drop collapse ability did not match the highest peak in the chromatogram (Figure 3.4). To verify that the peaks seen are best detected at 210 nm, we decided to modify the method using an additional gradient and additional wavelengths to obtain better resolution of our samples.

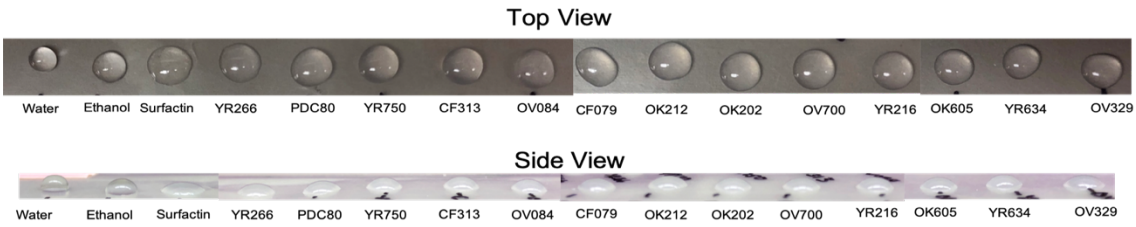

Figure 3.2: Drop collapse assay to verify reduced surface tension properties for the extracted biosurfactant samples from the 13 *Variovorax* strains. Purified *Bacillus subtilis* surfactin (Sigma) served as a positive control while water and ethanol served as negative controls. Ethanol was the solvent used to resuspend the samples. The results suggest that the extracted substance from the growing bacterial culture has biosurfactant properties. These results also show that *Variovorax* sp. PDC80 produces a biosurfactant despite the negative result for the atomized oil assay.

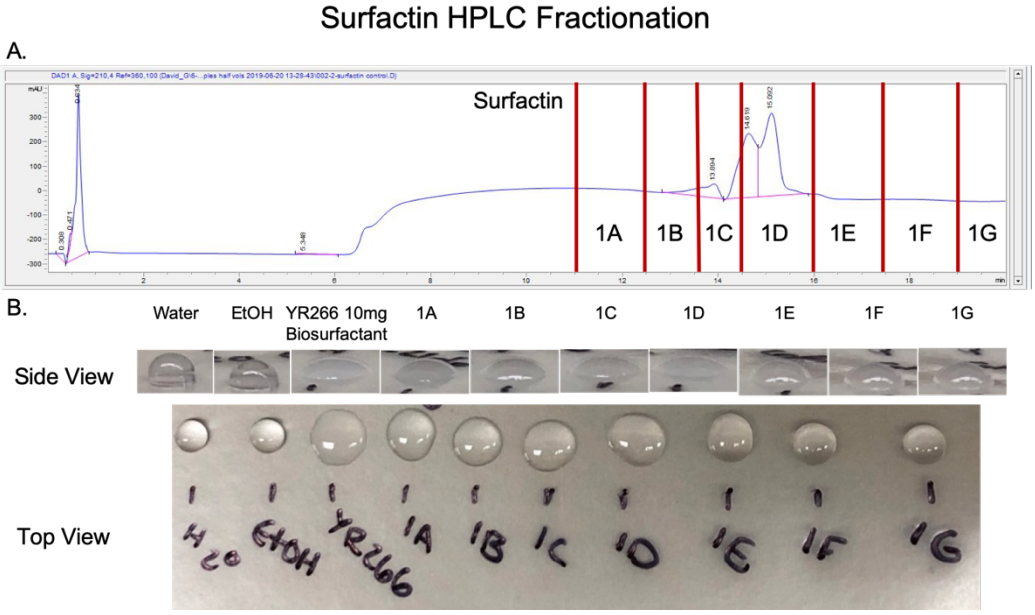

Figure 3.3: Surfactin HPLC fractionation spectra and drop collapse results. A) HPLC spectra showing the fraction collected based on certain time points (red lines). B) Drop collapse for the HPLC fractions. Water and EtOH served as negative controls. Crude extract of *Variovorax* sp. YR266 biosurfactant at a concentration of 10mg served as the positive control.

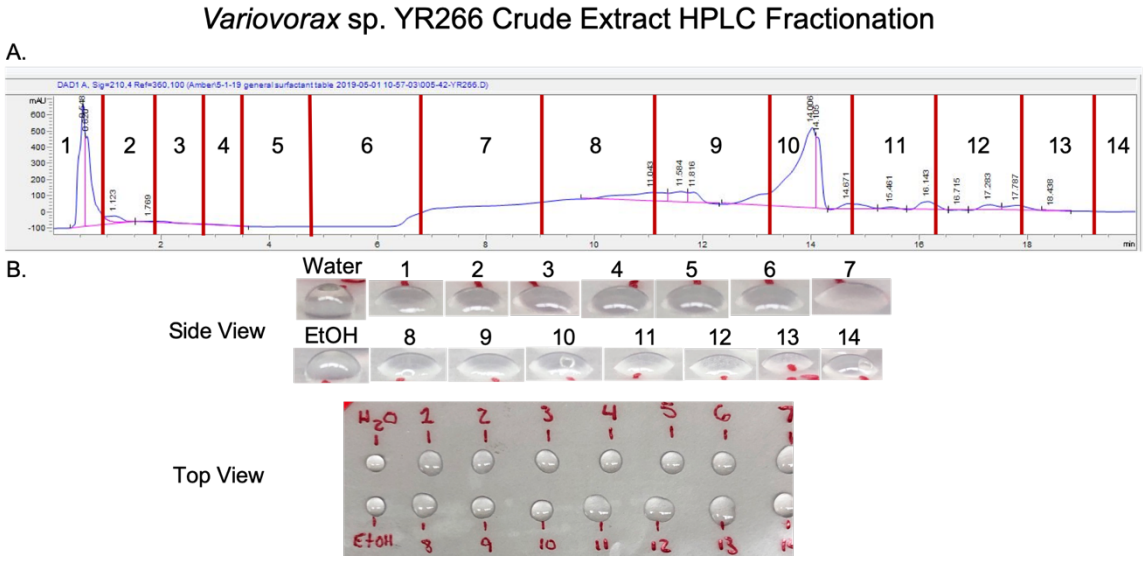

Figure 3.4: *Variovorax* sp. YR266 crude extract HPLC fractionation spectra and drop collapse results. A) HPLC spectra showing the fraction collected based on certain time points (red lines). B) Drop collapse for the HPLC fractions. Water and EtOH served as negative controls.

Using the new method, we found that our peaks eluted with better resolution, improving our results for the drop collapse ability (Figure 3.5). We also looked at the spectrum of wavelengths from 210nm to 600 nm to verify that our peaks were being seen at the best wavelength and that another peak was not being covered up. From this experiment, we found that 210nm provided the best resolution for our peaks.

MALDI- MSI

To begin to characterize the biosurfactant molecules, we began experiments using MALDI-MSI. Our goal for the project is to eventually use the MSI capabilities in order to visualize the biosurfactant molecules being produced from a growing *Variovorax* colony on a slide. MSI studies have been growing in recent years given its ability to map of the spatial distribution for a specific molecule in relation to a growing bacterial colony.[109,110] Other biosurfactants have been mapped using MSI and work well given their clear boundaries of secretion.[60,111,112]

The initial phase of our experiments focused on creating samples that would mitigate some of the common problems with the system. One of the biggest problems of MSI is sample flaking due to changes of vacuum pressure in the machine.[109] To combat this problem, we utilized agar that was poured directly onto a slide rather than being transferred from a petri dish to a target plate. This creates a sample that is securely attached to the slide and will remain as such once under vacuum pressure. Next, we needed to verify that the bacteria would grow and produce biosurfactants on a thin agar slide that is at the most 1mm high once dried.[109] We tested several thicknesses and found that we could put as little as 1mL of agar on a half sized slide and still have the bacteria grow and produce biosurfactants. Our next goal was to determine if *Variovorax* would still produce biosurfactants on a minimal media in order to try to limit the complexity of our agar surface. Therefore, we used MOPS minimal media with galactose as

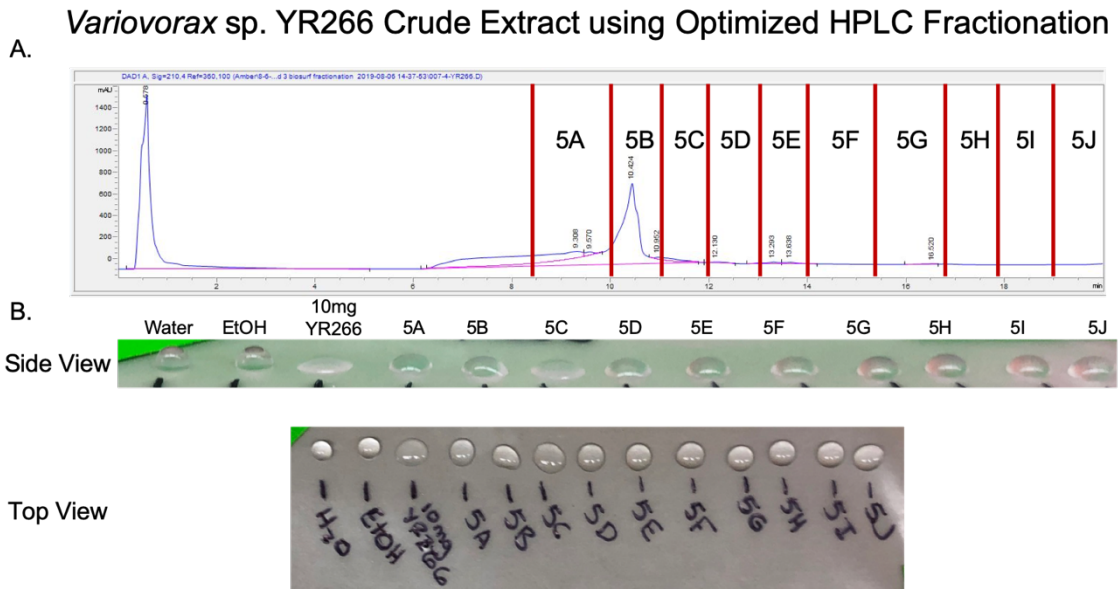

Figure 3.5: *Variovorax* sp. YR266 crude extract HPLC fractionation spectra and drop collapse results using optimized HPLC method. A) HPLC spectra showing the fraction collected based on certain time points (red lines). B) Drop collapse for the HPLC fractions. Water and EtOH served as negative controls. Crude extract of *Variovorax* sp. YR266 biosurfactant at a concentration of 10mg served as the positive control.

the carbon source. We found that biosurfactants are still produced on the minimal media. We also verified that the biosurfactants were detectable after desiccation by using the atomized oil assay to mist the slide with the colony after drying in the vacuum desiccator overnight (Figure 3.6A). Lastly, we needed a slide that was conductive in order to obtain quality spectras.[110] We obtained gold-plated slides in order to provide that conductive surface for the MALDI and found no issues using these slides for producing the samples (Figure 3.6B).

Once all of initial sample preparation optimization rounds were conducted, we were able to begin with optimization for matrix application and instrument paraments for the MALDI. MALDI requires the application of an organic matrix that will co-crystallize with the sample, allowing for ionization of the matrix-sample crystals when the laser is shot at the sample for detection.[113] Therefore, choosing a matrix that will crystallize with your sample is another key aspect for obtaining MALDI spectras. In order to limit the complexity of the spectras in the beginning, we started with taking spectras of standards, which were purified *Bacillus subtilis* surfactin and the crude biosurfactant extract for *Variovorax* sp. YR266, directly on a gold-plated glass slide without agar. We tried different matrices dissolved in different solvents to see how crystallization and detection differed. We found that CHCA dissolved in 50/50/0.1% of water/ACN/TFA provided the best spectra as we were able to see peaks for surfactin and the CHCA matrix peaks for calibration (Figure 3.7). When we used the same matrix for the *Variovorax* sp. YR266 samples on the gold-plated slide, we were not able to see peaks that were unique for only *Variovorax* sp. YR266. Given that we verified drop collapse activity in the sample before using MALDI, this suggests that our crude extract might not be at a high enough concentration to analyze the biosurfactant molecule.

We also began to analyze our standards on agar in order to look for unique agar peaks that may serve as a type of control to determine which peaks are the agar background noise and which are secreted molecules from the

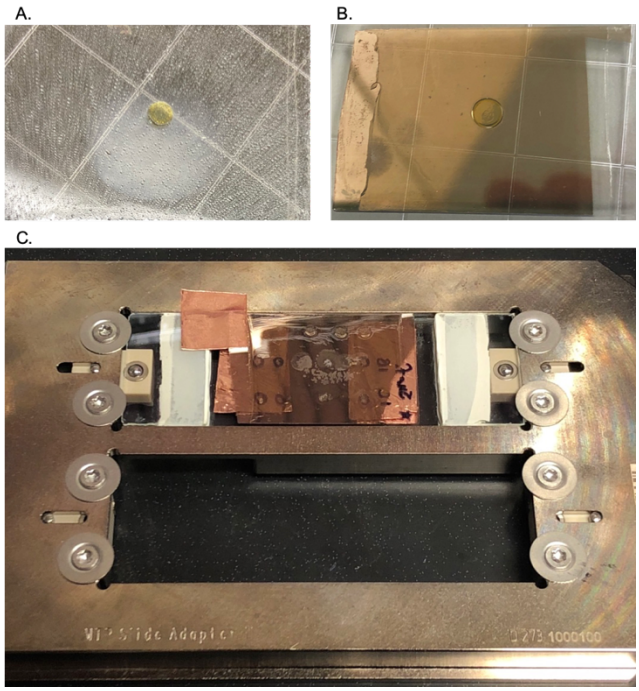

Figure 3.6: MALDI samples created from optimizing growing conditions. A) Desiccated slide showing the biosurfactant halo of *Variovorax* sp. YR266 grown on MOPS + 10mM galactose. B) Desiccated slide of *Variovorax* sp. YR266 before matrix has been applied. C) Desiccated slide of standards shown in the slide holder, ready for MALDI measurements.

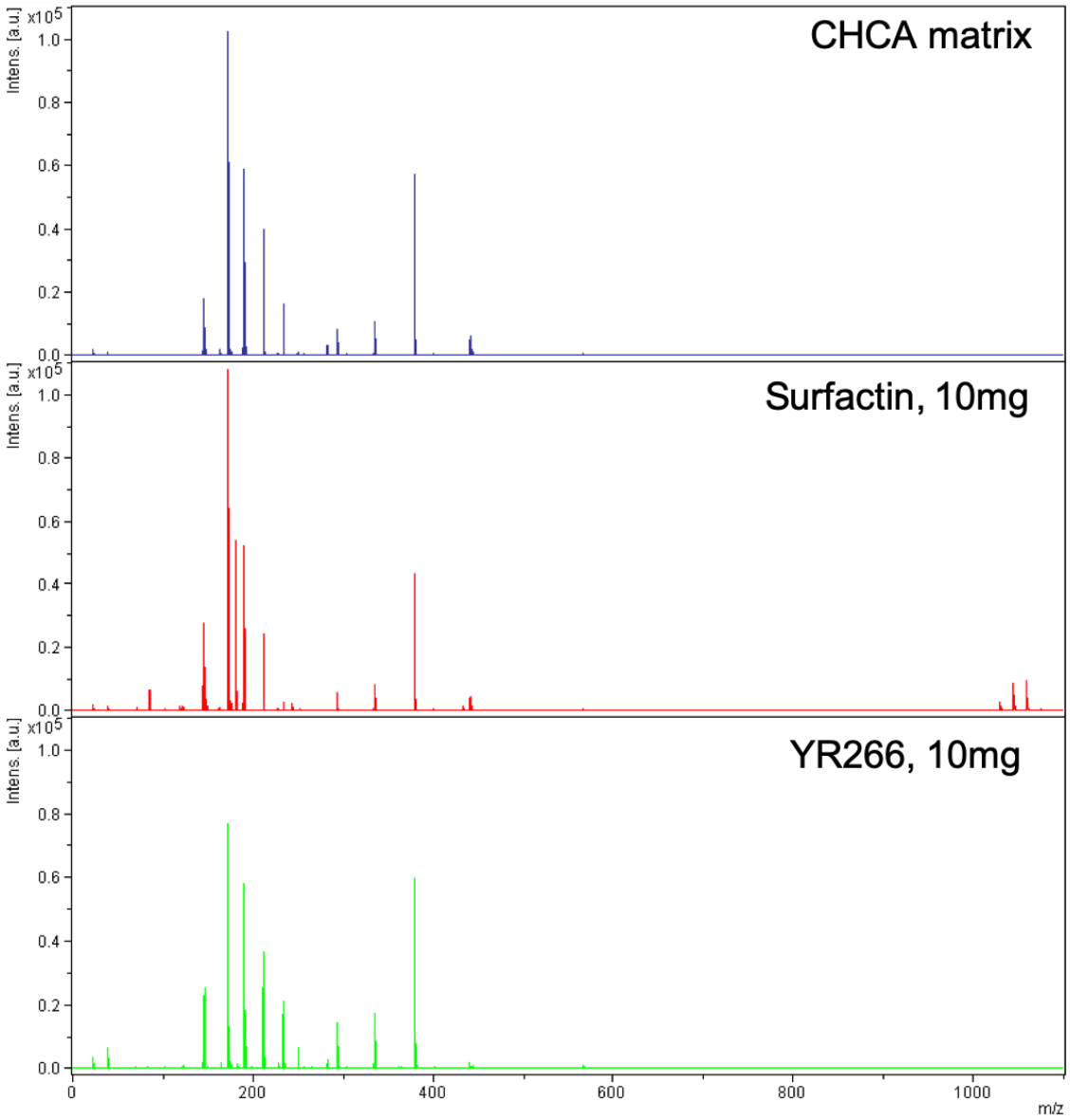

Figure 3.7: MALDI spectra for CHCA matrix (blue), 10mg surfactin (red), and 10mg *Variovorax* sp. YR266 (green) on gold-plated slide

growing bacterial colony. Using our current method, we were able to get a potential spectrum for agar (Figure 3.8). The spectrum is highly complex which is likely indicative of small molecules that are found within the agar sample. Spectra for both *Variovorax* sp. YR266 displayed similar results as on the gold-plated slide, again indicating a need for a more concentrated sample. Lastly, we were not able to obtain spectras for surfactin using the method due to a lack of crystallization on the agar. When the matrix was added through drop-cast (where a drop of matrix is spotted on the surface of your sample and allowed to dry), it appeared to interact with the agar and rather than creating crystals it almost appeared to rehydrate the agar. Therefore, different applications for the matrix need to be investigated.

Discussion

Biosurfactants are amphipathic molecules that have many uses within the microbiome, including antimicrobial, biofilm formation, and motility properties.[46] While biosurfactant production and structure have been characterized for other bacterial strains, including *P. aeruginosa* and *B. subtilis*, characterization to a similar degree has not been accomplished for any *Variovorax* strains.

We determined that the *Variovorax* species all produce biosurfactants. While all of the extracted biosurfactants have the ability to reduce surface tension, there is a lot of variety in how much each biosurfactant molecule collapses the drop and none do so as efficiently as surfactin. Additionally, the active fractions from HPLC fractionation did not necessarily correspond to the largest peak in the spectra. Both phenomena are likely due to the fact that we are using a general chloroform: methanol extraction that is used to extract all lipids, rather than only biosurfactants.[114] Therefore, other lipids are likely to be found within our samples, preventing a fully accurate measure of the biosurfactant portion within the sample, altering our initial results for the drop collapse and the HPLC active fractions.

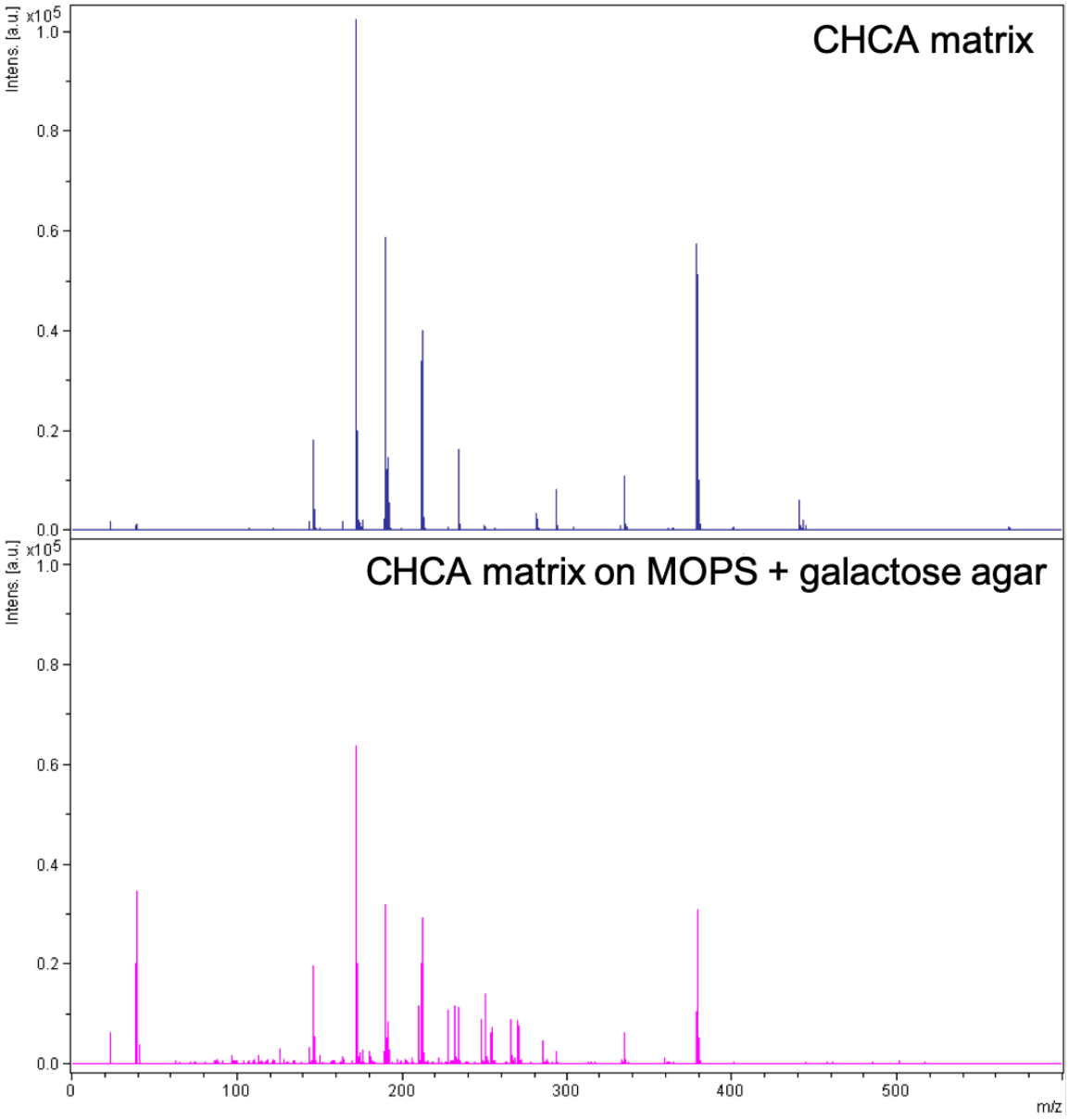

Figure 3.8: MALDI spectra comparing CHCA matrix on gold-plated slide without agar (blue) to CHCA matrix on agar (purple).

While characterization by MALDI is not complete, we have been able to begin optimization for MSI in the future. We have determined the best environment and sample preparations for our MALDI samples using *Variovorax* species as a colony growing on a slide and initial steps to recognize standards such as surfactin and agar with the CHCA matrix. We are still currently working on the best application of the matrix for imaging rather than drop-casting the matrix. Once final optimization has taken place with the MALDI, we will be able to obtain data using MSI.

Analysis of the MSI data could be difficult without a mass for the molecules. While our growing bacterial colony has been shown to produce a clear circle of biosurfactants, the molecular weight of biosurfactant molecules can range from low to high which can create a lot of variability when determining which peak is our biosurfactant compound within our spectra.[48,52] We are working on running our HPLC fractions with a more sensitive mass spectrometry in order to obtain a mass that can serve as an outside control for our MALDI-MSI data.

Future directions should focus on elucidating the role biosurfactants play in affecting the structure and abundance of microbes within the microbiome as it is currently limited. Recent research has found that biosurfactant molecules produced by *B. subtilis*, which are molecules known as surfactin, can be degraded by *Paenibacillus dendritiformis* and potentially used as territory markers to prevent other bacterial species from inhabiting their space.[60] However, few studies into how biosurfactants may play a role in interspecies relationships exist and could contribute to a deeper understanding of how natural products produced by bacteria within the microbiome can affect the community members and the plant itself. Future work to determine the specific properties of the biosurfactant and how it may impact other bacterial strains within the microbiome, such as antimicrobial properties or affecting surface attachment of other bacterial strains, is needed.

CHAPTER FOUR :
CONCLUSION

Investigating the role that a bacterial genus has within the microbiome is important to better understand the complex interactions within the plant microbiome. This study provides a unique look at thirteen *Variovorax* species that were isolated from the same plant host, *Populus*. However, differences in host genotype (*P. trichocarpa* and *P. deltoides*), location (Oregon, North Carolina, and Tennessee), the season collected (Spring and Fall), and isolation location of the species (with twelve endosphere isolates and one rhizosphere isolate), provided the ability to see how plant-associated *Variovorax* species potentially differ across time and space. While we found many genomic differences between the *Variovorax* species, we were able to identify a common natural product being produced, a biosurfactant.

Genomic comparisons of the *Variovorax* species revealed phylogenetic distributions that occupy unique niches within the genus as well as two closely related clusters. Additionally, the two closely related clusters have high similarities in their proteins, further demonstrating their relationship phylogenetically. When protein similarities were compared for the rest of the isolates, *Variovorax* sp. YR216, the only rhizosphere isolate, was revealed to have the least similarities in proteins compared to the rest of the isolates. This suggests potential functional differences between the isolates found within the endosphere compared to the rhizosphere. Other genomic analyses found differences in potential biosynthetic gene clusters as well as metabolic differences between the isolates.

Experimental analyses for the differences in the *Variovorax* species were also performed. Differences in growth medias and carbon sources revealed stark contrasts and preferences for the *Variovorax* isolates, with certain species preferring LB, a nutrient rich media, while other preferred R2A, a less nutritionally rich media. Additionally, while *Variovorax* sp. YR750 grew well on multiple carbon

sources, other species had specific preferences and no commonly preferred carbon source was found. Still another species, *Variovorax* sp. YR216, did not grow well on any carbon source tested. The *Variovorax* isolates were also found to influence the growth of other species when grown for pairwise interaction assays. These interactions could further demonstrate the metabolic similarities between the *Variovorax* isolates or similarities in natural product production. Further experiments are needed to elucidate whether the interactions demonstrate nutritional competition or evidence of natural products secreted by the *Variovorax* species.

Experiments were also performed to look at biosurfactant production and to begin characterizing the compounds produced by the *Variovorax* isolates. Through the descriptive atomized oil assay and the crude biosurfactant extractions, we found that all thirteen of the *Variovorax* species produce biosurfactant compounds. We next began to purify our compounds using HPLC fractionation where we were able to determine the fractions that had the ability to reduce surface tension effectively. Secondly, we began to optimize experiments for MSI using MALDI-TOF MS. We have determined a workflow for sample preparation for the MSI experiments and are beginning to work out the best methods for matrix application and adjusting MALDI instrument parameters that are sensitive for detecting our biosurfactant compound.

Our future goal for the biosurfactant characterization is to determine if the *Variovorax* species were producing the same biosurfactant compounds across the isolates as well as if the compounds are similar to any known biosurfactant compounds, such as surfactin or rhamnolipids. Additionally, understanding how these compounds may influence the plant microbiome by affecting colonization or the abundance of other microbes is of interest for the future. Biosurfactants are known to disrupt biofilms of some microbes as well as increase motility of others.[60,62,63] Furthermore, some biosurfactant compounds have antimicrobial properties.[61] Possible experiments to determine the properties of the

biosurfactants include adding the extracted biosurfactants to a glass or microfluidic surface to see if biofilm formation is inhibited for certain bacteria, determining if the biosurfactants have antimicrobial properties through disc diffusion assay, or through monitoring bacterial motility after a surface is coated with the extracted biosurfactant.

LIST OF REFERENCES

1 Reinhold-Hurek, B., Bunger, W., Burbano, C. S., Sabale, M. & Hurek, T. Roots shaping their microbiome: global hotspots for microbial activity. *Annu Rev Phytopathol* **53**, 403-424, doi:10.1146/annurev-phyto-082712-102342 (2015).

2 Torsvik, V., Ovreas, L. & Thingstad, T. F. Prokaryotic diversity--magnitude, dynamics, and controlling factors. *Science* **296**, 1064-1066, doi:10.1126/science.1071698 (2002).

3 Gaiero, J. R. *et al.* Inside the root microbiome: bacterial root endophytes and plant growth promotion. *Am J Bot* **100**, 1738-1750, doi:10.3732/ajb.1200572 (2013).

4 Berg, G., Grube, M., Schloter, M. & Smalla, K. Unraveling the plant microbiome: looking back and future perspectives. *Front Microbiol* **5**, 148, doi:10.3389/fmicb.2014.00148 (2014).

5 Shi, S. *et al.* Effects of selected root exudate components on soil bacterial communities. *FEMS Microbiol Ecol* **77**, 600-610, doi:10.1111/j.1574-6941.2011.01150.x (2011).

6 Bais, H. P., Weir, T. L., Perry, L. G., Gilroy, S. & Vivanco, J. M. The role of root exudates in rhizosphere interactions with plants and other organisms. *Annu Rev Plant Biol* **57**, 233-266, doi:10.1146/annurev.arplant.57.032905.105159 (2006).

7 Sasse, J., Martinoia, E. & Northen, T. Feed Your Friends: Do Plant Exudates Shape the Root Microbiome? *Trends Plant Sci* **23**, 25-41, doi:10.1016/j.tplants.2017.09.003 (2018).

8 Salah Ud-Din, A. I. M. & Roujeinikova, A. Methyl-accepting chemotaxis proteins: a core sensing element in prokaryotes and archaea. *Cell Mol Life Sci* **74**, 3293-3303, doi:10.1007/s00018-017-2514-0 (2017).

9 Bi, S. & Sourjik, V. Stimulus sensing and signal processing in bacterial chemotaxis. *Current Opinion in Microbiology* **45**, 22-29, doi:10.1016/j.mib.2018.02.002 (2018).

10 Sourjik, V. & Armitage, J. P. Spatial organization in bacterial chemotaxis. *EMBO Journal* **29**, 2724-2733, doi:10.1038/emboj.2010.178 (2010).

11 de Weert, S. *et al.* Flagella-driven chemotaxis towards exudate components is an important trait for tomato root colonization by *Pseudomonas fluorescens*. *Mol Plant Microbe Interact* **15**, 1173-1180, doi:10.1094/MPMI.2002.15.11.1173 (2002).

12 Allard-Massicotte, R. *et al. Bacillus subtilis* Early Colonization of *Arabidopsis thaliana* Roots Involves Multiple Chemotaxis Receptors. *MBio* **7**, e01664-01616, doi:10.1128/mBio.01664-16 (2016).

13 Bulgarelli, D., Schlaeppi, K., Spaepen, S., Ver Loren van Themaat, E. & Schulze-Lefert, P. Structure and functions of the bacterial microbiota of plants. *Annu Rev Plant Biol* **64**, 807-838, doi:10.1146/annurev-arplant-050312-120106 (2013).

14 Edwards, J. *et al.* Structure, variation, and assembly of the root-associated microbiomes of rice. *Proc Natl Acad Sci U S A* **112**, E911-920, doi:10.1073/pnas.1414592112 (2015).

15 Compant, S. *et al.* Endophytic colonization of *Vitis vinifera* L. by plant growth-promoting bacterium *Burkholderia* sp. strain PsJN. *Appl Environ Microbiol* **71**, 1685-1693, doi:10.1128/AEM.71.4.1685-1693.2005 (2005).

16 Garg, N. & Geetanjali. Symbiotic nitrogen fixation in legume nodules: process and signaling. A review. *Agronomy for Sustainable Development* **27**, 59-68, doi:10.1051/agro:2006030 (2007).

17 Reinhold-Hurek, B. & Hurek, T. Living inside plants: bacterial endophytes. *Curr Opin Plant Biol* **14**, 435-443, doi:10.1016/j.pbi.2011.04.004 (2011).

18 Goswami, D., Thakker, J. N., Dhandhukia, P. C. & Tejada Moral, M. Portraying mechanics of plant growth promoting rhizobacteria (PGPR): A review. *Cogent Food & Agriculture* **2**, 1127500, doi:10.1080/23311932.2015.1127500 (2016).

19 Lata, R., Chowdhury, S., Gond, S. K. & White, J. F., Jr. Induction of abiotic stress tolerance in plants by endophytic microbes. *Lett Appl Microbiol* **66**, 268-276, doi:10.1111/lam.12855 (2018).

20 Shameer, S. & Prasad, T. N. V. K. V. Plant growth promoting rhizobacteria for sustainable agricultural practices with special reference to biotic and abiotic stresses. *Plant Growth Regulation* **84**, 603-615, doi:10.1007/s10725-017-0365-1 (2018).

21 Glick, B. R. Bacteria with ACC deaminase can promote plant growth and help to feed the world. *Microbiol Res* **169**, 30-39, doi:10.1016/j.micres.2013.09.009 (2014).

22 Bonito, G. *et al.* Plant host and soil origin influence fungal and bacterial assemblages in the roots of woody plants. *Mol Ecol* **23**, 3356-3370, doi:10.1111/mec.12821 (2014).

23 Dukunde, A., Schneider, D., Schmidt, M., Veldkamp, E. & Daniel, R. Tree Species Shape Soil Bacterial Community Structure and Function in Temperate Deciduous Forests. *Frontiers in Microbiology* **10**, doi:10.3389/fmicb.2019.01519 (2019).

24 Fierer, N. Embracing the unknown: disentangling the complexities of the soil microbiome. *Nat Rev Microbiol* **15**, 579-590, doi:10.1038/nrmicro.2017.87 (2017).

25 Lauber, C. L., Hamady, M., Knight, R. & Fierer, N. Pyrosequencing-based assessment of soil pH as a predictor of soil bacterial community structure at the continental scale. *Appl Environ Microbiol* **75**, 5111-5120, doi:10.1128/AEM.00335-09 (2009).

26 Griffiths, R. I. *et al.* The bacterial biogeography of British soils. *Environ Microbiol* **13**, 1642-1654, doi:10.1111/j.1462-2920.2011.02480.x (2011).

27 Cederlund, H. *et al.* Soil carbon quality and nitrogen fertilization structure bacterial communities with predictable responses of major bacterial phyla. *Applied Soil Ecology* **84**, 62-68, doi:10.1016/j.apsoil.2014.06.003 (2014).

28 Sul, W. J. *et al.* Tropical agricultural land management influences on soil microbial communities through its effect on soil organic carbon. *Soil biology & biochemistry* **65**, 33-38 (2013).

29 Oliverio, A. M., Bradford, M. A. & Fierer, N. Identifying the microbial taxa that consistently respond to soil warming across time and space. *Glob Chang Biol* **23**, 2117-2129, doi:10.1111/gcb.13557 (2017).

30 Chaparro, J. M., Badri, D. V. & Vivanco, J. M. Rhizosphere microbiome assemblage is affected by plant development. *ISME J* **8**, 790-803, doi:10.1038/ismej.2013.196 (2014).

31 Monchgesang, S. *et al.* Natural variation of root exudates in *Arabidopsis thaliana*-linking metabolomic and genomic data. *Sci Rep* **6**, 29033, doi:10.1038/srep29033 (2016).

32 Micallef, S. A., Shiaris, M. P. & Colon-Carmona, A. Influence of *Arabidopsis thaliana* accessions on rhizobacterial communities and natural variation in root exudates. *J Exp Bot* **60**, 1729-1742, doi:10.1093/jxb/erp053 (2009).

33 Lareen, A., Burton, F. & Schafer, P. Plant root-microbe communication in shaping root microbiomes. *Plant Mol Biol* **90**, 575-587, doi:10.1007/s11103-015-0417-8 (2016).

34 Tyc, O., Song, C., Dickschat, J. S., Vos, M. & Garbeva, P. The Ecological Role of Volatile and Soluble Secondary Metabolites Produced by Soil Bacteria. *Trends Microbiol* **25**, 280-292, doi:10.1016/j.tim.2016.12.002 (2017).

35 Tuskan, G. A. *et al.* The genome of black cottonwood, *Populus trichocarpa* (Torr. & Gray). *Science* **313**, 1596-1604, doi:10.1126/science.1128691 (2006).

36 Gottel, N. R. *et al.* Distinct microbial communities within the endosphere and rhizosphere of *Populus deltoides* roots across contrasting soil types. *Appl Environ Microbiol* **77**, 5934-5944, doi:10.1128/AEM.05255-11 (2011).

37 Shakya, M. *et al.* A multifactor analysis of fungal and bacterial community structure in the root microbiome of mature *Populus deltoides* trees. *PLoS One* **8**, e76382, doi:10.1371/journal.pone.0076382 (2013).

38 Timm, C. M. *et al.* Metabolic functions of *Pseudomonas fluorescens* strains from *Populus deltoides* depend on rhizosphere or endosphere isolation compartment. *Front Microbiol* **6**, 1118, doi:10.3389/fmicb.2015.01118 (2015).

39 Timm, C. M. *et al.* Abiotic Stresses Shift Belowground *Populus*-Associated Bacteria Toward a Core Stress Microbiome. *mSystems* **3**, doi:10.1128/mSystems.00070-17 (2018).

40 Veach, A. M. *et al.* Rhizosphere microbiomes diverge among *Populus trichocarpa* plant-host genotypes and chemotypes, but it depends on soil origin. *Microbiome* **7**, 76, doi:10.1186/s40168-019-0668-8 (2019).

41 Bonito, G. *et al.* Fungal-Bacterial Networks in the *Populus* Rhizobiome Are Impacted by Soil Properties and Host Genotype. *Front Microbiol* **10**, 481, doi:10.3389/fmicb.2019.00481 (2019).

42 Ren, H., Wang, B. & Zhao, H. Breaking the silence: new strategies for discovering novel natural products. *Curr Opin Biotechnol* **48**, 21-27, doi:10.1016/j.copbio.2017.02.008 (2017).

43 Rutledge, P. J. & Challis, G. L. Discovery of microbial natural products by activation of silent biosynthetic gene clusters. *Nature Reviews Microbiology* **13**, 509, doi:10.1038/nrmicro3496 (2015).

44 Onaka, H., Mori, Y., Igarashi, Y. & Furumai, T. Mycolic acid-containing bacteria induce natural-product biosynthesis in *Streptomyces* species. *Appl Environ Microbiol* **77**, 400-406, doi:10.1128/AEM.01337-10 (2011).

45 Blair, P. M. *et al.* Exploration of the Biosynthetic Potential of the *Populus* Microbiome. *mSystems* **3**, e00045-00018, doi:10.1128/mSystems.00045-18 (2018).

46 Raaijmakers, J. M., De Bruijn, I., Nybroe, O. & Ongena, M. Natural functions of lipopeptides from *Bacillus* and *Pseudomonas*: more than surfactants and antibiotics. *FEMS Microbiol Rev* **34**, 1037-1062, doi:10.1111/j.1574-6976.2010.00221.x (2010).

47 Satpute, S. K., Banpurkar, A. G., Dhakephalkar, P. K., Banat, I. M. & Chopade, B. A. Methods for investigating biosurfactants and bioemulsifiers: a review. *Crit Rev Biotechnol* **30**, 127-144, doi:10.3109/07388550903427280 (2010).

48 Marchant, R. & Banat, I. M. Microbial biosurfactants: challenges and opportunities for future exploitation. *Trends Biotechnol* **30**, 558-565, doi:10.1016/j.tibtech.2012.07.003 (2012).

49 Chong, H. & Li, Q. Microbial production of rhamnolipids: opportunities, challenges and strategies. *Microb Cell Fact* **16**, 137, doi:10.1186/s12934-017-0753-2 (2017).

50 Dobler, L., Vilela, L. F., Almeida, R. V. & Neves, B. C. Rhamnolipids in perspective: gene regulatory pathways, metabolic engineering, production and technological forecasting. *N Biotechnol* **33**, 123-135, doi:10.1016/j.nbt.2015.09.005 (2016).

51 Banat, I. M. *et al.* Microbial biosurfactants production, applications and future potential. *Appl Microbiol Biotechnol* **87**, 427-444, doi:10.1007/s00253-010-2589-0 (2010).

52 Varjani, S. J. & Upasani, V. N. Critical review on biosurfactant analysis, purification and characterization using rhamnolipid as a model biosurfactant. *Bioresour Technol* **232**, 389-397, doi:10.1016/j.biortech.2017.02.047 (2017).

53 Ackerley, D. F. Cracking the Nonribosomal Code. *Cell Chem Biol* **23**, 535-537, doi:10.1016/j.chembiol.2016.05.001 (2016).

54 Hansen, D. B., Bumpus, S. B., Aron, Z. D., Kelleher, N. L. & Walsh, C. T. The loading module of mycosubtilin: an adenylation domain with fatty acid

selectivity. *J Am Chem Soc* **129**, 6366-6367, doi:10.1021/ja070890j (2007).

55 Caiazza, N. C., Shanks, R. M. & O'Toole, G. A. Rhamnolipids modulate swarming motility patterns of *Pseudomonas aeruginosa*. *J Bacteriol* **187**, 7351-7361, doi:10.1128/JB.187.21.7351-7361.2005 (2005).

56 Kearns, D. B. & Losick, R. Swarming motility in undomesticated *Bacillus subtilis*. *Mol Microbiol* **49**, 581-590, doi:10.1046/j.1365-2958.2003.03584.x (2003).

57 Davey, M. E., Caiazza, N. C. & O'Toole, G. A. Rhamnolipid surfactant production affects biofilm architecture in *Pseudomonas aeruginosa* PAO1. *J Bacteriol* **185**, 1027-1036, doi:10.1128/jb.185.3.1027-1036.2003 (2003).

58 Hofemeister, J. *et al.* Genetic analysis of the biosynthesis of non-ribosomal peptide- and polyketide-like antibiotics, iron uptake and biofilm formation by *Bacillus subtilis* A1/3. *Mol Genet Genomics* **272**, 363-378, doi:10.1007/s00438-004-1056-y (2004).

59 Charles Oluwaseun, A. *et al.* Characterization and optimization of a rhamnolipid from *Pseudomonas aeruginosa* C1501 with novel biosurfactant activities. *Sustainable Chemistry and Pharmacy* **6**, 26-36, doi:10.1016/j.scp.2017.07.001 (2017).

60 Luzzatto-Knaan, T., Melnik, A. V. & Dorrestein, P. C. Mass Spectrometry Uncovers the Role of Surfactin as an Interspecies Recruitment Factor. *ACS Chem Biol* **14**, 459-467, doi:10.1021/acschembio.8b01120 (2019).

61 Sachdev, D. P. & Cameotra, S. S. Biosurfactants in agriculture. *Appl Microbiol Biotechnol* **97**, 1005-1016, doi:10.1007/s00253-012-4641-8 (2013).

62 Dusane, D. H., Nancharaiah, Y. V., Zinjarde, S. S. & Venugopalan, V. P. Rhamnolipid mediated disruption of marine *Bacillus pumilus* biofilms. *Colloids Surf B Biointerfaces* **81**, 242-248, doi:10.1016/j.colsurfb.2010.07.013 (2010).

63 Irie, Y., O'Toole G, A. & Yuk, M. H. *Pseudomonas aeruginosa* rhamnolipids disperse *Bordetella bronchiseptica* biofilms. *FEMS Microbiol Lett* **250**, 237-243, doi:10.1016/j.femsle.2005.07.012 (2005).

64 Rodrigues, L. R., Banat, I. M., van der Mei, H. C., Teixeira, J. A. & Oliveira, R. Interference in adhesion of bacteria and yeasts isolated from explanted voice prostheses to silicone rubber by rhamnolipid biosurfactants. *J Appl Microbiol* **100**, 470-480, doi:10.1111/j.1365-2672.2005.02826.x (2006).

65 Satola, B., Wubbeler, J. H. & Steinbuchel, A. Metabolic characteristics of the species *Variovorax paradoxus*. *Appl Microbiol Biotechnol* **97**, 541-560, doi:10.1007/s00253-012-4585-z (2013).

66 Han, J. I. *et al.* Complete genome sequence of the metabolically versatile plant growth-promoting endophyte *Variovorax paradoxus* S110. *J Bacteriol* **193**, 1183-1190, doi:10.1128/JB.00925-10 (2011).

67 Leadbetter, J. R. & Greenberg, E. P. Metabolism of acyl-homoserine lactone quorum-sensing signals by *Variovorax paradoxus*. *J Bacteriol* **182**, 6921-6926, doi:10.1128/jb.182.24.6921-6926.2000 (2000).

68 Futamata, H., Nagano, Y., Watanabe, K. & Hiraishi, A. Unique kinetic properties of phenol-degrading *Variovorax* strains responsible for efficient trichloroethylene degradation in a chemostat enrichment culture. *Appl Environ Microbiol* **71**, 904-911, doi:10.1128/AEM.71.2.904-911.2005 (2005).

69 Mahan, K. M. *et al.* Iron-Dependent Enzyme Catalyzes the Initial Step in Biodegradation of N-Nitroglycine by *Variovorax* sp. Strain JS1663. *Appl Environ Microbiol* **83**, doi:10.1128/AEM.00457-17 (2017).

70 Posman, K. M., DeRito, C. M. & Madsen, E. L. Benzene Degradation by a *Variovorax* Species within a Coal Tar-Contaminated Groundwater Microbial Community. *Appl Environ Microbiol* **83**, e02658-02616, doi:10.1128/AEM.02658-16 (2017).

71 Snellinx, Z. Microbial consortia that degrade 2,4-DNT by interspecies metabolism: isolation and characterisation. *Biodegradation* **14**, 19-29, doi:10.1023/a:1023539104747 (2003).

72 Crombie, A. T. *et al.* Poplar phyllosphere harbors disparate isoprene-degrading bacteria. *Proc Natl Acad Sci U S A* **115**, 13081-13086, doi:10.1073/pnas.1812668115 (2018).

73 Jiang, F. *et al.* Multiple impacts of the plant growth-promoting rhizobacterium *Variovorax paradoxus* 5C-2 on nutrient and ABA relations of *Pisum sativum*. *J Exp Bot* **63**, 6421-6430, doi:10.1093/jxb/ers301 (2012).

74 Pereira, S. I. & Castro, P. M. Diversity and characterization of culturable bacterial endophytes from *Zea mays* and their potential as plant growth-promoting agents in metal-degraded soils. *Environ Sci Pollut Res Int* **21**, 14110-14123, doi:10.1007/s11356-014-3309-6 (2014).

75 Sessitsch, A., Reiter, B. & Berg, G. Endophytic bacterial communities of field-grown potato plants and their plant-growth-promoting and antagonistic abilities. *Can J Microbiol* **50**, 239-249, doi:10.1139/w03-118 (2004).

76 Gamalero, E. & Glick, B. R. Bacterial Modulation of Plant Ethylene Levels. *Plant Physiology* **169**, 13-22, doi:10.1104/pp.15.00284 (2015).

77 Aufrecht, J. A. *et al.* Quantifying the Spatiotemporal Dynamics of Plant Root Colonization by Beneficial Bacteria in a Microfluidic Habitat. *Advanced Biosystems* **2**, n/a-n/a, doi:10.1002/adbi.201800048 (2018).

78 Chen, L., Dodd, I. C., Theobald, J. C., Belimov, A. A. & Davies, W. J. The rhizobacterium *Variovorax paradoxus* 5C-2, containing ACC deaminase, promotes growth and development of *Arabidopsis thaliana* via an ethylene-dependent pathway. *J Exp Bot* **64**, 1565-1573, doi:10.1093/jxb/ert031 (2013).

79 Sun, S. L. *et al.* The Plant Growth-Promoting Rhizobacterium *Variovorax boronicumulans* CGMCC 4969 Regulates the Level of Indole-3-Acetic Acid Synthesized from Indole-3-Acetonitrile. *Appl Environ Microbiol* **84**, e00298-00218, doi:10.1128/AEM.00298-18 (2018).

80 Vurukonda, S. S., Vardharajula, S., Shrivastava, M. & Sk, Z. A. Enhancement of drought stress tolerance in crops by plant growth promoting rhizobacteria. *Microbiol Res* **184**, 13-24, doi:10.1016/j.micres.2015.12.003 (2016).

81 Neidhardt, F. C., Bloch, P. L. & Smith, D. F. Culture medium for enterobacteria. *J Bacteriol* **119**, 736-747 (1974).

82 Varghese, N. J. *et al.* Microbial species delineation using whole genome sequences. *Nucleic Acids Res* **43**, 6761-6771, doi:10.1093/nar/gkv657 (2015).

83 Dereeper, A. *et al.* Phylogeny.fr: robust phylogenetic analysis for the non-specialist. *Nucleic Acids Research* **36**, W465-W469, doi:10.1093/nar/gkn180 (2008).

84 Blin, K. *et al.* antiSMASH 4.0-improvements in chemistry prediction and gene cluster boundary identification. *Nucleic Acids Res* **45**, W36-W41, doi:10.1093/nar/gkx319 (2017).

85 Vesth, T., Lagesen, K., Acar, O. & Ussery, D. CMG-biotools, a free workbench for basic comparative microbial genomics. *PLoS One* **8**, e60120, doi:10.1371/journal.pone.0060120 (2013).

86 Parsek, M. R. & Greenberg, E. P. Acyl-homoserine lactone quorum sensing in gram-negative bacteria: a signaling mechanism involved in associations with higher organisms. *Proc Natl Acad Sci U S A* **97**, 8789-8793, doi:10.1073/pnas.97.16.8789 (2000).

87 Schaefer, A. L. *et al.* LuxR- and luxI-type quorum-sensing circuits are prevalent in members of the *Populus deltoides* microbiome. *Appl Environ Microbiol* **79**, 5745-5752, doi:10.1128/AEM.01417-13 (2013).

88 Patankar, A. V. & Gonzalez, J. E. Orphan LuxR regulators of quorum sensing. *FEMS Microbiol Rev* **33**, 739-756, doi:10.1111/j.1574-6976.2009.00163.x (2009).

89 Darzins, A. & Russell, M. A. Molecular genetic analysis of type-4 pilus biogenesis and twitching motility using *Pseudomonas aeruginosa* as a model system – a review. *Gene* **192**, 109-115, doi:10.1016/s0378-1119(97)00037-1 (1997).

90 Whitchurch, C. B. *et al.* Characterization of a complex chemosensory signal transduction system which controls twitching motility in *Pseudomonas aeruginosa*. *Mol Microbiol* **52**, 873-893, doi:10.1111/j.1365-2958.2004.04026.x (2004).

91 Hickman, J. W., Tifrea, D. F. & Harwood, C. S. A chemosensory system that regulates biofilm formation through modulation of cyclic diguanylate levels. *Proc Natl Acad Sci U S A* **102**, 14422-14427, doi:10.1073/pnas.0507170102 (2005).

92 Martínez-Núñez, M. A. & López, V. E. L. y. Nonribosomal peptides synthetases and their applications in industry. *Sustainable Chemical Processes* **4**, 13, doi:10.1186/s40508-016-0057-6 (2016).

93 Schoner, T. A. *et al.* Aryl Polyenes, a Highly Abundant Class of Bacterial Natural Products, Are Functionally Related to Antioxidative Carotenoids. *Chembiochem* **17**, 247-253, doi:10.1002/cbic.201500474 (2016).

94 Schulz-Bohm, K., Martin-Sanchez, L. & Garbeva, P. Microbial Volatiles: Small Molecules with an Important Role in Intra- and Inter-Kingdom Interactions. *Front Microbiol* **8**, 2484, doi:10.3389/fmicb.2017.02484 (2017).

95 Stevenson, G., Andrianopoulos, K., Hobbs, M. & Reeves, P. R. Organization of the *Escherichia coli* K-12 gene cluster responsible for production of the extracellular polysaccharide colanic acid. *J Bacteriol* **178**, 4885-4893, doi:10.1128/jb.178.16.4885-4893.1996 (1996).

96 Ziemert, N. *et al.* The natural product domain seeker NaPDoS: a phylogeny based bioinformatic tool to classify secondary metabolite gene diversity. *PLoS One* **7**, e34064, doi:10.1371/journal.pone.0034064 (2012).

97 Nishizawa, T. *et al.* Polyketide synthase gene coupled to the peptide synthetase module involved in the biosynthesis of the cyclic heptapeptide microcystin. *J Biochem* **127**, 779-789, doi:10.1093/oxfordjournals.jbchem.a022670 (2000).

98 Schikora, A., Schenk, S. T. & Hartmann, A. Beneficial effects of bacteria-plant communication based on quorum sensing molecules of the N-acyl homoserine lactone group. *Plant Mol Biol* **90**, 605-612, doi:10.1007/s11103-016-0457-8 (2016).

99 Schaefer, A. L. *et al.* A LuxR Homolog in a Cottonwood Tree Endophyte That Activates Gene Expression in Response to a Plant Signal or Specific Peptides. *MBio* **7**, e01101-01116, doi:10.1128/mBio.01101-16 (2016).

100 Subramoni, S. *et al.* Bacterial Subfamily of LuxR Regulators That Respond to Plant Compounds. *Appl Environ Microbiol* **77**, 4579-4588, doi:10.1128/aem.00183-11 (2011).

101 Coutinho, B. G. *et al.* A plant-responsive bacterial-signaling system senses an ethanolamine derivative. *Proc Natl Acad Sci U S A* **115**, 9785-9790, doi:10.1073/pnas.1809611115 (2018).

102 Whiteley, M., Diggle, S. P. & Greenberg, E. P. Progress in and promise of bacterial quorum sensing research. *Nature* **551**, 313-320, doi:10.1038/nature24624 (2017).

103 Kurth, C., Schieferdecker, S., Athanasopoulou, K., Seccareccia, I. & Nett, M. Variochelins, Lipopeptide Siderophores from *Variovorax boronicumulans* Discovered by Genome Mining. *Journal of Natural Products* **79**, 865-872, doi:10.1021/acs.jnatprod.5b00932 (2016).

104 Robertson, A. W. *et al.* Isolation of Imaqobactin, an Amphiphilic Siderophore from the Arctic Marine Bacterium *Variovorax* Species

RKJM285. *J Nat Prod* **81**, 858-865, doi:10.1021/acs.jnatprod.7b00943 (2018).

105 Jamieson, W. D., Pehl, M. J., Gregory, G. A. & Orwin, P. M. Coordinated surface activities in *Variovorax paradoxus* EPS. *BMC Microbiol* **9**, 124, doi:10.1186/1471-2180-9-124 (2009).

106 Burch, A. Y., Shimada, B. K., Browne, P. J. & Lindow, S. E. Novel high-throughput detection method to assess bacterial surfactant production. *Appl Environ Microbiol* **76**, 5363-5372, doi:10.1128/AEM.00592-10 (2010).

107 Varjani, S. J. & Upasani, V. N. Carbon spectrum utilization by an indigenous strain of *Pseudomonas aeruginosa* NCIM 5514: Production, characterization and surface active properties of biosurfactant. *Bioresour Technol* **221**, 510-516, doi:10.1016/j.biortech.2016.09.080 (2016).

108 Sivapathasekaran, C., Mukherjee, S., Samanta, R. & Sen, R. High-performance liquid chromatography purification of biosurfactant isoforms produced by a marine bacterium. *Anal Bioanal Chem* **395**, 845-854, doi:10.1007/s00216-009-3023-2 (2009).

109 Yang, J. Y. *et al.* Primer on agar-based microbial imaging mass spectrometry. *J Bacteriol* **194**, 6023-6028, doi:10.1128/JB.00823-12 (2012).

110 Watrous, J. D. & Dorrestein, P. C. Imaging mass spectrometry in microbiology. *Nat Rev Microbiol* **9**, 683-694, doi:10.1038/nrmicro2634 (2011).

111 Yang, Y. L., Xu, Y., Straight, P. & Dorrestein, P. C. Translating metabolic exchange with imaging mass spectrometry. *Nat Chem Biol* **5**, 885-887, doi:10.1038/nchembio.252 (2009).

112 Hoefler, B. C. *et al.* Enzymatic resistance to the lipopeptide surfactin as identified through imaging mass spectrometry of bacterial competition. *Proc Natl Acad Sci U S A* **109**, 13082-13087, doi:10.1073/pnas.1205586109 (2012).

113 Hankin, J. A., Barkley, R. M. & Murphy, R. C. Sublimation as a method of matrix application for mass spectrometric imaging. *J Am Soc Mass Spectrom* **18**, 1646-1652, doi:10.1016/j.jasms.2007.06.010 (2007).

114 Heyd, M. *et al.* Development and trends of biosurfactant analysis and purification using rhamnolipids as an example. *Anal Bioanal Chem* **391**, 1579-1590, doi:10.1007/s00216-007-1828-4 (2008).

VITA

Jennifer A. Childers obtained a Bachelor of Science degree in Biology from Samford University in 2015. Before entering graduate school, she worked in agriculture biotechnology where she helped to prepare seeds and sample materials for field trials. During her graduate work, she conducted research as part of the Plant Microbe Interfaces group at Oak Ridge National Laboratory with Dr. Jennifer Morrell-Falvey. With her Master of Science degree from the Genome Science and Technology program, her goal is to return to the biotechnology sector for research.